isvr Institute of Sound and Vibration Research

Estimation of Acoustic Source Strength by Inverse Methods: Part I: Conditioning of the Inverse Problem

S.H. Yoon and P.A. Nelson

ISVR Technical Report No 278

October 1998

University of Southampton

SCIENTIFIC PUBLICATIONS BY THE ISVR

Technical Reports are published to promote timely dissemination of research results by ISVR personnel. This medium permits more detailed presentation than is usually acceptable for scientific journals. Responsibility for both the content and any opinions expressed rests entirely with the author(s).

Technical Memoranda are produced to enable the early or preliminary release of information by ISVR personnel where such release is deemed to the appropriate. Information contained in these memoranda may be incomplete, or form part of a continuing programme; this should be borne in mind when using or quoting from these documents.

Contract Reports are produced to record the results of scientific work carried out for sponsors, under contract. The ISVR treats these reports as confidential to sponsors and does not make them available for general circulation. Individual sponsors may, however, authorize subsequent release of the material.

UNIVERSITY OF SOUTHAMPTON

INSTITUTE OF SOUND AND VIBRATION RESEARCH

FLUID DYNAMICS AND ACOUSTICS GROUP

Estimation of Acoustic Source Strength by Inverse Methods: Part I: Conditioning of the Inverse Problem

by

P A Nelson and S H Yoon

ISVR Technical Report No. 278

October 1998

Authorized for issue by
Professor P A Nelson
Group Chairman

CONTENTS

FIGURES

Figure 12. Singular values of the matrix **H** for the model of Figure 5: circle: $r_{ms}=0.5r_{ss}$ ($\kappa(\mathbf{H})=5.90$), plus: $r_{ms}=2r_{ss}$ ($\kappa(\mathbf{H})=5.06\text{x}10^{2}$), x-mark: $r_{ms}=3r_{ss}$ ($\kappa(\mathbf{H})=7.50\text{x}10^{3}$), star: $r_{ms}=30r_{ss}$ ($\kappa(\mathbf{H})=2.16\text{x}10^{15}$).

Figure 13. Resolution capability of the singular value discarding technique for the 9 monopole source and 9 microphone model (Figure 5) with the change of the distance r_{ms} and the singular values discarded. Graphs show the magnitude of $\mathbf{q}_o$ (m^3/s^{-1}) as a function of position x (m) (1st column: discarding no singular value, 2nd column: discarding the last singular value, 3rd column: discarding the last 3 singular values, 4th column: discarding the last 5 singular values): $kr_{ss}=0.366$ (=200Hz): (a) 10% noise, (b) 20% noise.

Figure 14. Resolution capability of the Tikhonov regularisation technique for the 9 monopole source and 9 microphone model (Figure 5) with the change of the distance r_{ms} and the regularisation parameter. Graphs show the magnitude of $\mathbf{q}_o$ (m^3/s^{-1}) as a function of position x (m). (1st column: $\beta=0$, 2nd column: $\beta=1\text{x}10^{-5}$, 3rd column: $\beta=1\text{x}10^{-2}$, 4th column: $\beta=10$): $kr_{ss}=0.366$ (=200Hz): (a) 10% noise, (b) 20% noise.

Figure 15. Row elements of the matrices $\mathbf{U}^{\mathrm{H}}$ and $\mathbf{V}^{\mathrm{H}}$ for the source/sensor geometry illustrated in Figure 5 with $r_{ms}=3$m ($r_{ms}/r_{ss}=30$) and $kr_{ss}=0.183$ (100Hz). The left hand column shows the singular values of **H** corresponding to the rows of $\mathbf{U}^{\mathrm{H}}$ and $\mathbf{V}^{\mathrm{H}}$.

Figure 16. Row elements of the matrices $\mathbf{U}^{\mathrm{H}}$ and $\mathbf{V}^{\mathrm{H}}$ for the source/sensor geometry illustrated in Figure 5 with $r_{ms}=0.3$m ($r_{ms}/r_{ss}=3$) and $kr_{ss}=0.183$ (100Hz). The left hand column shows the singular values of **H** corresponding to the rows of $\mathbf{U}^{\mathrm{H}}$ and $\mathbf{V}^{\mathrm{H}}$.

ABSTRACT

This report deals with the discrete inverse problem in acoustics. It is assumed that a number of acoustic sources are located at known spatial positions and that the acoustic pressure is measured at a number of spatial positions in the radiated field. The transfer functions relating the strengths of the acoustic sources to the radiated pressures are also assumed known. In principle, the strengths of the acoustic sources can be deduced from the measured acoustic pressures by inversion of this matrix of transfer functions. The accuracy of source strength reconstruction (in the presence of noise which contaminates the measured pressures) is crucially dependent on the conditioning of the matrix to be inverted. This report examines the conditioning of this inverse problem, particularly with regard to the geometry and number of sources and measurement positions and the non-dimensional frequency. A preliminary investigation is also presented of methods such as Tikhonov regularisation and singular value discarding which can improve the accuracy of source strength reconstruction in poorly conditioned cases. Results are also presented which enable the solution of the inverse problem when the time histories of the acoustic sources are time-stationary random processes and the spectra and cross-spectra are measured at a number of positions in the radiated field. The report illustrates the possibilities and limitations of the use of inverse methods in the deduction of acoustic source strength from radiated field measurements.

1. INTRODUCTION

The estimation of the strength of acoustic sources from measurements of their radiated field is a subject which has been studied extensively by acoustical engineers. The most widely studied problem is that of estimating the angular location of a source relative to an array of sensors, specifically with regard to the detection of sources of underwater sound [1]. Here however, we consider in detail the problem of estimating the strength of the components of a source distribution whose position in space is either known or can be modelled with reasonable accuracy. This problem is of most relevance to engineers who wish to better understand sources of sound in order to reduce their output. Considerable effort was directed towards this problem during the 1970's when researchers first became particularly concerned with the accurate location of sources associated with jet engines. For example, Billingsley and Kinns [2] developed an "acoustic telescope" which made use of an array of microphones whose outputs were weighted depending on an assumed source position. These workers deduced the relationship between the power spectrum of the resulting output signal and the cross power spectral distribution of an assumed line source upon which the array is focused. Another approach was that taken by Fisher *et al* [3] who derived a relationship between the source strength distribution associated with an uncorrelated line source and the cross correlation functions evaluated between microphones located on a polar arc surrounding the source. This work forms the basis of the "polar correlation" technique. Fisher *et al* demonstrated that the technique is intrinsically unable to resolve sources separated by less than one half of an acoustic wavelength. A further approach to the source reconstruction problem was that taken by Maynard *et al* [4] who introduced the use of near field acoustic holography (NAH). In this case, the field impinging on an array that is placed close to the region of the source is decomposed into its constituent plane wave components through the use of a wavenumber transform. Subsequent extrapolation of this field to the plane of the source then follows from the solution of the Helmholtz equation in

the wavenumber domain. By undertaking measurements in the near field source components can be resolved which are separated by distances of much less than one half wavelength. The implementation of this technique is described in more detail by Veronesi and Maynard [5] and its practical use has been clearly described by Hald [6, 7] and Ginn and Hald [8].

In addition to these approaches to the problem, another method for reconstructing an estimate of the source distribution has been used by a number of workers. For example, in a later report on the polar correlation technique, Tester and Fisher [9] described an "automatic source breakdown technique" which relied on a pre-supposed model of the jet noise source distribution. Tester and Fisher proceeded to find the strengths associated with their model which minimised the difference between the measured cross spectra of the microphone array signals and those predicted by their model. A very similar approach to the source identification problem was later taken by Filippi *et al* [10]. These workers introduced a numerical technique which again enabled identification of an *a priori* chosen model for the source distribution. The essence of this approach was to find the distribution of source strength used in the model which minimised a cost function which quantified the mean square error between the measured field and the output of the model. The models used by Filippi *et al* consisted of either a decomposition of the radiated field into spherical harmonics or a discretised representation of the source distribution in a Kirchoff-Helmholtz representation of the source and sound field. As an example, these workers modelled the radiation from a vibrating beam, expressed the field in terms of spherical harmonics up to sixth order, and deduced the source strengths associated with nineteen discrete elements of the beam. They introduced 10% random error into their simulated measurements and studied the accuracy to which the source distribution could be reconstructed as a function of the position of the measurements made. They noted that the technique became more accurate as the measurement array was moved closer to the source distribution. The connection between this type of approach and that of NAH was made by Veronesi and

Maynard [11] who also used a discretised version of a Kirchoff-Helmholtz representation of source distributions but for those with arbitrary geometry. A matrix of transfer functions was then defined which related the strengths of these discrete sources to the acoustic pressure at a number of field points. This matrix was then expressed in terms of its singular value decomposition (SVD) and Veronesi and Maynard pointed out the similarity between the matrix operations in the SVD and those used in NAH. The generality of the SVD as a method of relating source and field was subsequently exploited by Borgiotti [12], Photiadis [13] and Elliott and Johnson [14], all of whom made use of the technique to define a set of spatially orthogonal source strength distributions and study the efficiency of their radiation to the far field. Kim and Lee [15] also used the SVD in connection with a Kirchoff-Helmholtz representation of the source and radiated field which enabled the field at a number of discrete points to be expressed in terms of the source distribution at a number of discrete points. These authors used the SVD in order to deal with any ill-conditioning of the matrix to be inverted. The technique was found to be successful in practice when applied to the radiation from a cabinet mounted loudspeaker.

More recently, Stoughton and Strait [16] have studied the use of the least squares method for the identification of the distribution of source strength associated with a line source and Grace *et al* [17, 18] have studied the aeroacoustic inverse problem of identifying the unsteady surface pressure along a streamlined airfoil from the measurement of the radiated sound field. Grace *et al* made use of Tikhonov regularisation in order to deal with ill-conditioning, although the choice of the regularisation parameter in the inversion process was made arbitrarily. Fisher and Holland [19] have also recently made use of the same approach in the identification of the sources of shock-cell noise in supersonic jets, although no explicit use was made of regularisation techniques.

In summary therefore, there appear to have been two main categories of approach to the source reconstruction problem. The first category relies on "Fourier transform" relationships between source and field, whilst the second uses what may be described as a

"model based" approach although, as pointed out by Veronesi and Maynard [11], there is a close connection between the two methods. It is the second, more general, approach that we study further in this work. In particular we show that, once the sources are well modelled, the accuracy of source strength reconstruction using this technique is determined entirely by the properties of the matrix of transfer functions used in the model which describes the source and field and the amount of measurement noise. We again use the singular value decomposition to both evaluate the errors in source reconstruction with a given microphone array and to improve the accuracy of reconstruction. In this report, we firstly reintroduce the analytical basis of the technique with a view to maximising the accessibility of the work to acoustical engineers. Furthermore, we concentrate on the effect of the geometry of the problem on its conditioning and guidelines are given for the design of microphone arrays which enable good results to be achieved. The report begins with an introduction to the general least squares estimation problem and sets out the analytical framework for subsequent analysis using the SVD and other techniques for improving estimation accuracy, such as Tikhonov regularisation. We also introduce within this framework a convenient technique for the analysis of source distributions having a stationary random output as a function of time. In particular we deduce the relationship between cross spectra measured between microphones in the radiated field and the cross spectral distribution of the modelled sources.

The main results of this report demonstrate the influence of the geometrical arrangement of sources and sensors on the conditioning of the problem and in particular the improvements in conditioning produced by making measurements in the near field of the sources. Furthermore, results are presented which show the power of singular value discarding and Tikhonov regularisation in enabling good results to be achieved even when the problem is poorly conditioned. We also show, however, that the use of singular value discarding also has consequences for the spatial resolution of the technique, and we explain our results in terms of the radiation efficiency of a set of spatially orthogonal source

strength distributions which are defined naturally by the SVD. In subsequent reports, we deal in more detail with methods for improving the conditioning of problems of this type which do not require *a priori* knowledge of the source strength distribution or measurement noise. In particular, we focus on the use of generalised cross validation [20] for choosing either the regularisation parameter or the singular values to be discarded.

2. THEORETICAL BACKGROUND

2.1 THE LEAST SQUARES SOLUTION TO THE ESTIMATION PROBLEM

The basis of the approach is illustrated in Figure 1 which shows a diagrammatic representation of both the real source and measurement array and the modelled sources and modelled measurement array. The output of the model can be written as

$$\mathbf{p} = \mathbf{H}\,\mathbf{q} \quad , \tag{1}$$

where the vector **p** is a complex vector of Fourier transforms of model microphone outputs and the matrix **H** is a matrix of complex frequency response functions relating the source strengths in the model to the output of the model microphones. The vector **q** is a complex vector of source strength Fourier transforms whose values we wish to determine. Note that in general the nature of the model sources is described by the elements of the matrix **H**. Thus for example, if the chosen source model were a combination of monopole and dipole type sources, then the respective monopole and dipole strengths would be defined in the vector **q** whilst the radiation patterns of these sources would be defined by the elements of the matrix **H**. When written in full equation (1) becomes

$$\begin{bmatrix} p_1(\omega) \\ p_2(\omega) \\ . \\ . \\ p_M(\omega) \end{bmatrix} = \begin{bmatrix} H_{11}(j\omega) & H_{12}(j\omega) & . & . & H_{1N}(j\omega) \\ H_{21}(j\omega) & H_{22}(j\omega) & . & . & H_{2N}(j\omega) \\ . & . & & & . \\ . & . & & & . \\ H_{M1}(j\omega) & H_{M2}(j\omega) & . & . & H_{MN}(j\omega) \end{bmatrix} \begin{bmatrix} q_1(\omega) \\ q_2(\omega) \\ . \\ . \\ q_N(\omega) \end{bmatrix} , \tag{2}$$

where we have assumed that the vector **p** is of order M (i.e. there are M microphones), the vector **q** is of order N (i.e. there are N sources), and the matrix **H** is of order $M \times N$. Furthermore we assume that we have an M'th order vector of *measured* complex Fourier transforms given by

$$\hat{\mathbf{p}}^{\mathrm{T}} = [\hat{p}_1(\omega)\, \hat{p}_2(\omega) \ldots \hat{p}_M(\omega)] \ . \tag{3}$$

It is now assumed that the measured vector of pressures is equal to the modelled vector of pressures plus a vector **e** whose components represent the departure of the measurements from the model and which may include, for example, the effect of contaminating noise. Thus

$$\hat{\mathbf{p}} = \mathbf{H}\, \mathbf{q} + \mathbf{e} \ . \tag{4}$$

We now seek the solution for the vector **q** of modelled source strengths that ensures the "best fit" of the modelled sound field to the measured data. The traditional approach to problems of this type is to find the "least squares" solution for the complex source strength vector **q** which ensures the minimisation of the sum of the squared errors ("residuals") between the measured microphone outputs and the model microphone outputs. It is also generally assumed that the number of microphones M is greater than or equal to the number of sources N. The complex error vector can be written as

$$\mathbf{e} = \hat{\mathbf{p}} - \mathbf{p} = \hat{\mathbf{p}} - \mathbf{H}\,\mathbf{q} \quad , \tag{5}$$

and the cost function for minimisation is defined by

$$J = \sum_{m=1}^{M} |e_m(\omega)|^2 = \mathbf{e}^{\mathrm{H}}\mathbf{e} \quad , \tag{6}$$

where the superscript H denotes the Hermitian transpose of a vector (i.e. the complex conjugate of the transposed vector). It is readily shown [21] that the optimal estimate of the source strength vector that minimises this function is given by

$$\mathbf{q}_o = [\mathbf{H}^{\mathrm{H}}\,\mathbf{H}]^{-1}\,\mathbf{H}^{\mathrm{H}}\,\hat{\mathbf{p}} \quad . \tag{7}$$

It can also be shown that this minimum is unique provided that the matrix $\mathbf{H}^{\mathrm{H}}\mathbf{H}$ is positive definite, i.e. provided that $\mathbf{q}^{\mathrm{H}}\,\mathbf{H}^{\mathrm{H}}\mathbf{H}\,\mathbf{q} > 0$ for all vectors $\mathbf{q} \neq \mathbf{0}$. Since, in this problem, $\mathbf{q}^{\mathrm{H}}\,\mathbf{H}^{\mathrm{H}}\,\mathbf{H}\,\mathbf{q} = \hat{\mathbf{p}}^{\mathrm{H}}\,\hat{\mathbf{p}}$, which is the sum of the squared magnitudes of the Fourier spectra of the model sources, we are assured of the positive definitiveness of $\mathbf{H}^{\mathrm{H}}\mathbf{H}$ and the existence of a unique minimum. Note that when the number of microphones M is made equal to the number of modelled sources N, the solution reduces to $\mathbf{q}_o = \mathbf{H}^{-1}\,\hat{\mathbf{p}}$. When M is less than N, no solution exists for the source strength vector unless some further constraint is introduced [21]. As we will demonstrate below, the usefulness of the least squares solution given by equation (7) depends crucially on the properties of the matrix to be inverted. It may be the case that the matrix to be inverted is either singular or "nearly singular" and it is in cases such as this that the singular value decomposition (SVD) is of such great utility.

2.2 THE SINGULAR VALUE DECOMPOSITION

Now note that we can decompose any arbitrary complex matrix such as the matrix **H** into the form [22, 23, 24]

$$\mathbf{H} = \mathbf{U}\,\Sigma\,\mathbf{V}^{\mathrm{H}} \ , \tag{8}$$

where the $M \times N$ matrix Σ is given by

$$\Sigma = \begin{bmatrix} \sigma_1 & 0 & . & . & 0 \\ 0 & \sigma_2 & & & 0 \\ . & . & & & . \\ 0 & 0 & . & . & \sigma_N \\ 0 & 0 & & & 0 \\ . & . & & & . \\ 0 & 0 & . & . & 0 \end{bmatrix} , \tag{9}$$

and comprises the matrix of N singular values σ_n of the $M \times N$ matrix **H**. The matrix **U** is of order $M \times M$ and its columns comprise the left singular vectors of the matrix **H**, whilst the matrix **V** is of order $N \times N$ and its columns comprise the right singular vectors of the matrix **H**. The matrices **U** and **V** are unitary and have the properties

$$\mathbf{U}^{\mathrm{H}}\,\mathbf{U} = \mathbf{U}\,\mathbf{U}^{\mathrm{H}} = \mathbf{I} \ , \tag{10}$$

$$\mathbf{V}^{\mathrm{H}}\,\mathbf{V} = \mathbf{V}\,\mathbf{V}^{\mathrm{H}} = \mathbf{I} \ . \tag{11}$$

It is usual to arrange the singular values $\sigma_1, \sigma_2 \ldots \sigma_N$ in descending order of magnitude in the matrix defined by equation (9). As we will see below, these singular values are of great utility in the analysis of our problem. One particularly important property of the

singular values is that the ratio of the maximum singular value of a matrix to the minimum singular value of the matrix can be used to define the "condition number" of the matrix. We will return to this below.

2.3 THE LEAST SQUARES SOLUTION IN TERMS OF THE SINGULAR VALUE DECOMPOSITION

Returning to the least squares solution for the optimal source strength Fourier spectra when the number of microphones M exceeds the number of source elements N, it follows from equation (7) that

$$\mathbf{q}_o = \left[\mathbf{H}^H\mathbf{H}\right]^{-1} \mathbf{H}^H\hat{\mathbf{p}} \ . \tag{12}$$

Substitution of the SVD given by equation (8) results in

$$\mathbf{q}_o = \left[\left(\mathbf{U}\ \Sigma\ \mathbf{V}^H\right)^H \left(\mathbf{U}\ \Sigma\ \mathbf{V}^H\right)\right]^{-1} \left(\mathbf{U}\ \Sigma\ \mathbf{V}^H\right)^H \hat{\mathbf{p}} \ , \tag{13}$$

which can be expanded to give

$$\mathbf{q}_o = \left[\mathbf{V}\ \Sigma^H\ \mathbf{U}^H\ \mathbf{U}\ \Sigma\ \mathbf{V}^H\right]^{-1} \mathbf{V}\ \Sigma^H\ \mathbf{U}^H\ \hat{\mathbf{p}} \ , \tag{14}$$

Use of equations (10) and (11) and the identity $(\mathbf{ABC})^{-1} = \mathbf{C}^{-1}\ \mathbf{B}^{-1}\ \mathbf{A}^{-1}$ then shows that

$$\mathbf{q}_o = \mathbf{V}\left[\Sigma^H\ \Sigma\right]^{-1} \Sigma^H\ \mathbf{U}^H\ \hat{\mathbf{p}} \ . \tag{15}$$

Since the matrix Σ has the particular form defined in equation (9), equation (15) can be rewritten in terms of the matrix Σ^+ which is defined by

$$\Sigma^{+} = \left[\Sigma^{H}\,\Sigma\right]^{-1}\Sigma^{H} \quad . \tag{16}$$

This yields the solution which can be written compactly as

$$\mathbf{q}_o = \mathbf{V}\,\Sigma^{+}\,\mathbf{U}^{H}\,\hat{\mathbf{p}} \quad . \tag{17}$$

Note that the matrix Σ^{+} takes a particular form. It follows from equation (9) that

$$\Sigma^{H}\Sigma = \begin{bmatrix} \sigma_1^{\,2} & 0 & . & . & 0 \\ 0 & \sigma_2^{\,2} & . & . & . \\ . & . & & & . \\ 0 & 0 & . & . & \sigma_N^{\,2} \end{bmatrix} , \tag{18}$$

which is simply a diagonal matrix of the squared singular values which, when inverted, yields a diagonal matrix having terms of the form $(1/\sigma_n^{\,2})$. Therefore when the inverse of $\Sigma^{H}\Sigma$ is multiplied by Σ^{H} this yields simply

$$\Sigma^{+} = \begin{bmatrix} 1/\sigma_1 & 0 & . & . & 0 & 0 & . & 0 \\ 0 & 1/\sigma_2 & & & . & . & & . \\ . & . & & & . & . & & . \\ 0 & 0 & . & 1/\sigma_N & 0 & 0 & . & 0 \end{bmatrix} . \tag{19}$$

The matrix Σ^{+} is usually referred to as the "pseudo inverse" of the matrix Σ. One very important observation follows from equation (17). That is, any very small singular value will result in large elements of the matrix Σ^{+}. This in turn will yield very large values of the solution. A traditionally used approach to the stabilisation of this solution is simply to discard any small singular values of the matrix **H** in computing the source strength estimate

given by equation (17). Thus, for example, one simply discards the $N-D$ smallest singular values and thus sets the terms $(1/\sigma_N,\ 1/\sigma_{N-1}\ ..\ 1/\sigma_{D+1})$ to zero in the above matrix. We will refer to this matrix as Σ_D^+ where D denotes the number of singular values left after discarding.

2.4 TIKHONOV REGULARISATION

Another approach to stabilising the solution given by equation (17) follows from an alternative definition of the cost function for minimisation. Rather than simply minimising the sum of the squared errors between the measured microphone spectra and the model output spectra we minimise a cost function which also penalises the sum of the squared model source strengths. We therefore choose to minimise

$$J_R = \mathbf{e}^H\mathbf{e} + \beta\,\mathbf{q}^H\mathbf{q}\ , \tag{20}$$

where β is a small regularisation parameter.

It is again readily shown [23] that this cost function is minimised by the optimal estimate of the source strength Fourier spectra defined by

$$\mathbf{q}_R = \left[\mathbf{H}^H\,\mathbf{H}\ +\ \beta\ \mathbf{I}\right]^{-1}\mathbf{H}^H\,\hat{\mathbf{p}}\ . \tag{21}$$

Use of the SVD in this expression then shows that

$$\mathbf{q}_R = \left[\mathbf{V}\ \Sigma^H\ \Sigma\ \mathbf{V}^H\ +\ \beta\ \mathbf{I}\right]^{-1}\mathbf{V}\,\Sigma^H\,\mathbf{U}^H\,\hat{\mathbf{p}}\ . \tag{22}$$

In view of equation (11) this can also be written as

$$\mathbf{q}_R = \left[\mathbf{V}\left[\Sigma^{\mathrm{H}}\,\Sigma + \beta\,\mathbf{I}\right]\mathbf{V}^{\mathrm{H}}\right]^{-1}\mathbf{V}\,\Sigma^{\mathrm{H}}\,\mathbf{U}^{\mathrm{H}}\,\hat{\mathbf{p}}\ , \tag{23}$$

and again using equation (11) demonstrates that the solution can be reduced to

$$\mathbf{q}_R = \mathbf{V}\left[\Sigma^{\mathrm{H}}\,\Sigma + \beta\,\mathbf{I}\right]^{-1}\Sigma^{\mathrm{H}}\,\mathbf{U}^{\mathrm{H}}\,\hat{\mathbf{p}}\ . \tag{24}$$

Now note that the matrix to be inverted can be written as

$$\left[\Sigma^{\mathrm{H}}\,\Sigma + \beta\,\mathbf{I}\right] = \begin{bmatrix} \sigma_1^{\,2}+\beta & 0 & . & . & 0 \\ 0 & \sigma_2^{\,2}+\beta & . & . & 0 \\ . & . & & & . \\ 0 & 0 & . & . & \sigma_N^{\,2}+\beta \end{bmatrix}. \tag{25}$$

The regularisation parameter β is therefore shown to be useful in increasing the value of all the diagonal terms in the matrix. Thus any particularly small squared singular value will effectively be increased by the regularisation parameter β. In computing the solution we can also define a "regularised" pseudo inverse matrix given by

$$\Sigma_R^{+} = \left[\Sigma^{\mathrm{H}}\,\Sigma + \beta\,\mathbf{I}\right]^{-1}\Sigma^{\mathrm{H}} = \begin{bmatrix} \dfrac{\sigma_1}{\sigma_1^{\,2}+\beta} & 0 & . & . & 0 & 0 & . & . & 0 \\ 0 & \dfrac{\sigma_2}{\sigma_2^{\,2}+\beta} & . & & 0 & 0 & & & 0 \\ . & . & & . & . & . & & & . \\ . & . & & . & . & . & & & . \\ 0 & 0 & . & \dfrac{\sigma_N}{\sigma_N^{\,2}+\beta} & 0 & 0 & . & . & 0 \end{bmatrix}, \tag{26}$$

which enables our solution to be written in the compact form

$$\mathbf{q}_o = \mathbf{V}\, \Sigma_R^{+}\, \mathbf{U}^{H}\, \hat{\mathbf{p}} \ . \tag{27}$$

The optimal estimate of the source strength Fourier spectra follows simply from undertaking a singular value decomposition of the matrix **H** of transfer functions used in the model. Later we will consider the effect of regularisation in computing the solution for the source strengths.

2.5 THE SOLUTION FOR THE SOURCE STRENGTH CROSS SPECTRA

The analysis leading to equations (17) and (27) above is perfectly general and applicable in practice to acoustic sources that have a deterministic time history (either periodic or transient, for example) which therefore readily yield measurable Fourier spectra. However, in practical acoustics one is often faced with a source strength distribution which has a time dependence which can be regarded as random with stationary statistical properties. In this case the spectra of the measured acoustic pressure will often be estimated from a series of finite length time histories of random data. Thus, for example, we can define the Fourier spectrum of the i'th segment of data of duration T as measured at the m'th microphone by

$$\hat{p}_{mi}(\omega) = \int_o^T p_{mi}(t)\, e^{-j\omega t}\, dt \ , \tag{28}$$

and similarly define the complex vector $\hat{\mathbf{p}}_i$ whose elements are $\hat{p}_{mi}(\omega)$. In addition, we can assume that the modelled acoustic source strengths have analogously defined Fourier spectra $q_{ni}(\omega)$ which comprise the complex vector $\mathbf{q}_i$. One can then deduce the optimal estimate $\mathbf{q}_{i_o}$ which minimises the mean square errors between the i'th Fourier spectra

measured at the microphones and those deduced from the model. That is we assume $\mathbf{p}_i = \mathbf{H}\,\mathbf{q}_i$ and minimise $\mathbf{e}_i^{\mathrm{H}}\,\mathbf{e}_i$ where $\mathbf{e}_i = \mathbf{p}_i - \hat{\mathbf{p}}_i$. This shows that

$$\mathbf{q}_{i_O} = \left[\mathbf{H}^{\mathrm{H}}\mathbf{H}\right]^{-1}\mathbf{H}^{\mathrm{H}}\,\hat{\mathbf{p}}_i \quad . \tag{29}$$

We may now formally define the matrix of optimally estimated acoustic source strength auto- and cross-spectra by

$$\mathbf{S}_{qq_O} = \lim_{T \to \infty} E\left[\frac{1}{T}\,\mathbf{q}_{i_O}\,\mathbf{q}_{i_O}^{\mathrm{H}}\right] \quad , \tag{30}$$

where $E[\ ]$ denotes the expectation operator. It then follows from substitution of equation (29) into equation (30) that

$$\mathbf{S}_{qq_O} = \left\{(\mathbf{H}^{\mathrm{H}}\mathbf{H})^{-1}\,\mathbf{H}^{\mathrm{H}}\right\}\,\mathbf{S}_{\hat{p}\hat{p}}\,\left\{(\mathbf{H}^{\mathrm{H}}\mathbf{H})^{-1}\,\mathbf{H}^{\mathrm{H}}\right\}^{\mathrm{H}} \quad , \tag{31}$$

where we have defined the matrix of measured acoustic pressure auto- and cross-spectra by

$$\mathbf{S}_{\hat{p}\hat{p}} = \lim_{T \to \infty} E\left[\frac{1}{T}\,\hat{\mathbf{p}}_i\,\hat{\mathbf{p}}_i^{\mathrm{H}}\right] \quad . \tag{32}$$

In practice of course, this latter quantity is estimated by, for example, averaging over a large (but finite) number of data segments of duration T.

Note that it is also possible to argue, that the solution given by equation (31) can be written in terms of the SVD of the matrix $\mathbf{H}$. It follows directly from the argument presented in Section 2.3 that we may write

$$\mathbf{S}_{qq_O} = \left\{\mathbf{V}\Sigma^{+}\,\mathbf{U}^{\mathrm{H}}\right\}\,\mathbf{S}_{\hat{p}\hat{p}}\,\left\{\mathbf{V}\,\Sigma^{+}\,\mathbf{U}^{\mathrm{H}}\right\}^{\mathrm{H}} \quad , \tag{33}$$

where we may choose to discard a number of small singular values of the pseudo-inverse matrix Σ^+ and replace this matrix by Σ_D^+ or indeed, replace Σ^+ by its Tikhonov regularised counterpart denoted above by Σ_R^+.

3. CONDITIONING OF ACOUSTIC TRANSFER FUNCTION MATRICES

3.1 SENSITIVITY OF SOLUTIONS TO CONDITION NUMBER

Assume for the moment that we are interested in solving the inverse problem posed when the number of microphones M is equal to the number of source elements N (i.e. the matrix $\mathbf{H}$ is square and the solution is given by equation (4)). The sensitivity of the solution for $\mathbf{q}$ to small deviations or errors in $\mathbf{H}$ and $\hat{\mathbf{p}}$ is determined by the condition number of the matrix $\mathbf{H}$ which has to be inverted. This condition number is usually defined as

$$\kappa(\mathbf{H}) = \|\mathbf{H}\| \, \|\mathbf{H}^{-1}\| \ , \tag{34}$$

where $\|\mathbf{H}\|$ denotes the 2-norm of the matrix $\mathbf{H}$. (See reference [22] for the definitions of the various matrix norms.) The 2-norm of $\mathbf{H}$ turns out to be equal to the largest singular value of $\mathbf{H}$ and is also equal to the square root of the largest eigenvalue of the matrix $\mathbf{H}^H \mathbf{H}$ [22]. Thus, in terms of the singular value decomposition, $\|\mathbf{H}\| = \sigma_{max}$ and $\|\mathbf{H}^{-1}\| = 1/\sigma_{min}$, where σ_{max} and σ_{min} are respectively the maximum and minimum singular values of $\mathbf{H}$. Therefore, for a square matrix $\mathbf{H}$,

$$\kappa(\mathbf{H}) = \sigma_{max}/\sigma_{min} \ . \tag{35}$$

A simple argument can be used to demonstrate the importance of the condition number to the sensitivity of the solution $\mathbf{q}_o = \mathbf{H}^{-1}\,\hat{\mathbf{p}}$ to errors, for example, in the measurement of $\hat{\mathbf{p}}$. Assume for the moment that small deviations of $\mathbf{p}$ produce small deviations $\delta\mathbf{q}$ in the solution. That is, we assume that $\mathbf{H}\,\mathbf{q} = \mathbf{p}$ and that

$$\mathbf{H}(\mathbf{q} + \delta\,\mathbf{q}) = (\mathbf{p} + \delta\,\mathbf{p}) \quad . \tag{36}$$

A useful property of the matrix 2-norm is that $\|\mathbf{A}\,\mathbf{B}\| \le \|\mathbf{A}\|\,\|\mathbf{B}\|$ for two matrices $\mathbf{A}$ and $\mathbf{B}$ [22]. Since $\delta\,\mathbf{q} = \mathbf{H}^{-1}\,\delta\,\mathbf{p}$ it therefore follows that $\|\delta\,\mathbf{q}\| \le \|\mathbf{H}^{-1}\|\,\|\delta\,\mathbf{p}\|$. It also follows that $\|\mathbf{p}\| \le \|\mathbf{H}\|\,\|\mathbf{q}\|$ and therefore we can write

$$\|\delta\,\mathbf{q}\|\,\|\mathbf{p}\| \le \|\mathbf{H}\|\,\|\mathbf{H}^{-1}\|\,\|\delta\,\mathbf{p}\|\,\|\mathbf{q}\| \quad , \tag{37}$$

and using the definition of the condition number shows that

$$\frac{\|\delta\,\mathbf{q}\|}{\|\mathbf{q}\|} \le \kappa\,(\mathbf{H})\,\frac{\|\delta\,\mathbf{p}\|}{\|\mathbf{p}\|} \quad . \tag{38}$$

This important and well established result demonstrates clearly that the sensitivity of the solution for $\mathbf{q}$ is determined by the condition number of the matrix $\mathbf{H}$ to be inverted; a large ratio of maximum to minimum singular value of $\mathbf{H}$ will greatly amplify small perturbations in $\mathbf{p}$. In practical terms, extraneous noise introduced into the measurement of the acoustic pressure will have a disproportionately large effect on the solution for the source strength vector $\mathbf{q}$ if the matrix is "badly conditioned" with a large $\kappa(\mathbf{H})$. A more sophisticated analysis [22] can be used to study the sensitivity of the solution to errors in the matrix $\mathbf{H}$ itself and again, the errors produced in the solution are found to be in proportion to the condition number of $\mathbf{H}$.

When the matrix $\mathbf{H}$ is not square, its condition number is defined by

$$\kappa(\mathbf{H}) = \|\mathbf{H}\| \, \|\mathbf{H}^{+}\| \ , \tag{39}$$

where $\mathbf{H}^{+} = (\mathbf{H}^{H} \, \mathbf{H})^{-1} \, \mathbf{H}^{H}$ is the pseudo-inverse of $\mathbf{H}$. The 2-norm of $\mathbf{H}^{+}$ is given by $1/\sigma_n$, where σ_n is the smallest non-zero singular value of $\mathbf{H}$, and therefore the condition number of a non-square matrix can be written as

$$\kappa(\mathbf{H}) = \sigma_{\max}/\sigma_n \ . \tag{40}$$

It is also easy to show, by using a very similar argument to that presented above for the case of a square matrix $\mathbf{H}$, that the sensitivity to errors in the measurement $\hat{\mathbf{p}}$ of the "least squares" solution given by equation (7) is also described by equation (38) but with the condition number defined by equation (39).

It is also important to evaluate the dependence upon condition number of the sensitivity of the solution given by equation (31) for the matrix of auto-spectra and cross-spectra of acoustic source strength, this being evaluated from the matrix of auto-spectra and cross-spectra of measured acoustic pressures. In this case, using $\mathbf{H}^{+} = (\mathbf{H}^{H} \, \mathbf{H})^{-1} \, \mathbf{H}^{H}$ to again denote the pseudo-inverse of $\mathbf{H}$, we can write the solution given by equation (1) in the form

$$\mathbf{S}_{qq} = \mathbf{H}^{+} \, \mathbf{S}_{pp} \, \mathbf{H}^{+H} \ , \tag{41}$$

and now assuming that errors $\delta \mathbf{S}_{pp}$ in the measured pressure cross-spectral matrix result in errors $\delta \mathbf{S}_{qq}$ in the source strength cross-spectral matrix shows that

$$\delta \mathbf{S}_{qq} = \mathbf{H}^{+} \, \delta \mathbf{S}_{pp} \, \mathbf{H}^{+H} \ . \tag{42}$$

We can thus use the matrix norm property to write $\|\delta \mathbf{S}_{qq_o}\| \leq \|\mathbf{H}^{+}\| \, \|\delta \mathbf{S}_{pp}\| \, \|\mathbf{H}^{+H}\|$. Again using the property of matrix norms in equation (41) shows that $\|\mathbf{S}_{pp}\| \leq \|\mathbf{H}\| \, \|\mathbf{S}_{qq}\| \, \|\mathbf{H}^{H}\|$ and we can therefore write

$$\|\delta \mathbf{S}_{qq}\| \, \|\mathbf{S}_{pp}\| \leq \|\mathbf{H}\| \, \|\mathbf{H}^{+}\| \, \|\mathbf{H}^{H}\| \, \|\mathbf{H}^{+H}\| \, \|\mathbf{S}_{qq}\| \, \|\delta \mathbf{S}_{pp}\| \ , \tag{43}$$

and therefore that

$$\frac{\|\delta \mathbf{S}_{qq}\|}{\|\mathbf{S}_{qq}\|} \leq \kappa(\mathbf{H}) \ \kappa(\mathbf{H}^{H}) \frac{\|\delta \mathbf{S}_{pp}\|}{\|\mathbf{S}_{pp}\|} \ . \tag{44}$$

We have again used the definition of the condition number of a non-square matrix $\mathbf{H}$ given by equation (39), above, and since the ratio of maximum to minimum singular values of $\mathbf{H}$ will be the same as those of $\mathbf{H}^{H}$, we can write

$$\frac{\|\delta \mathbf{S}_{qq}\|}{\|\mathbf{S}_{qq}\|} \leq \kappa(\mathbf{H})^{2} \frac{\|\delta \mathbf{S}_{pp}\|}{\|\mathbf{S}_{pp}\|} \ . \tag{45}$$

This result, which is generalisation to non-square matrices $\mathbf{H}$ of that first derived in reference [25], demonstrates clearly that the estimation of acoustic source strength auto- and cross-spectra is even more sensitive to errors (because of squared condition number) in the measurement of pressure spectra than when simply attempting to estimate source strength Fourier spectra. This is perhaps not surprising since the auto-spectrum is proportional to the square of the Fourier spectrum and one would expect errors to be equivalently amplified. However, estimating the power spectrum is often the only option in practice and this result emphasises the need to deal effectively with poorly conditioned

problems through the use of regularisation methods such as Tikhonov regularisation and singular value discarding.

3.2 PRINCIPAL FACTORS AFFECTING CONDITION NUMBER

A simple model will be used to give an initial indication of the factors which affect the condition number of the matrix to be inverted in deducing acoustic source strength for field measurements. Consider the two-source/two-microphone geometry illustrated in Figure 2. In this case the matrix **H** can be written as

$$\mathbf{H} = \frac{j\omega\rho_o}{4\pi}\begin{bmatrix} \dfrac{e^{-jkr_{11}}}{r_{11}} & \dfrac{e^{-jkr_{12}}}{r_{12}} \\ \dfrac{e^{-jkr_{21}}}{r_{21}} & \dfrac{e^{-jkr_{22}}}{r_{22}} \end{bmatrix} , \tag{46}$$

where $k = \omega/c_o$ is the wavenumber, ω the angular frequency and c_o the sound speed. Volume velocity has been used to quantify the strengths of the sources which are assumed to be point monopoles. A convenient way to find analytical expressions for the singular values of this matrix is to follow the procedure outlined in reference [26] and find the eigenvalues λ from the roots of

$$|\lambda \mathbf{I} - \mathbf{H}^{\mathrm{H}} \mathbf{H}| = 0 \ . \tag{47}$$

A little algebra [21] shows that these are given by

$$\lambda = \frac{\omega^2 \rho_o{}^2}{32\pi^2}\left[P \pm \sqrt{\left[P^2 - 4Q + 8R\cos kS\right]}\right] , \tag{48}$$

where the geometrical parameters P, Q, R and S are given by

$$P = \frac{1}{r_{11}^{\,2}} + \frac{1}{r_{12}^{\,2}} + \frac{1}{r_{21}^{\,2}} + \frac{1}{r_{22}^{\,2}} \ ,$$

$$Q = \frac{1}{r_{11}^{\,2}\, r_{22}^{\,2}} + \frac{1}{r_{12}^{\,2}\, r_{21}^{\,2}} \ ,$$

$$R = 1/r_{11}\, r_{12}\, r_{21}\, r_{22} \ ,$$

$$S = (r_{12} + r_{21}) - (r_{11} + r_{22}) \ . \tag{49}$$

The condition number of **H** can thus be expressed as

$$\kappa(\mathbf{H})^2 = \frac{P + \sqrt{\left[P^2 - 4Q + 8R\cos kS\right]}}{P - \sqrt{\left[P^2 - 4Q + 8R\cos kS\right]}} \ . \tag{50}$$

Note first that the frequency dependence of the condition number is encapsulated by the term cos kS in the above expression. This is obviously an oscillatory function of frequency since S will be fixed for a given geometrical arrangement of sources and sensors. The frequency dependence of the condition number is illustrated in Figure 3 for a particular arrangement of two sources and two sensors. The condition number in this case clearly exhibits an oscillatory behaviour with peaks in the condition number occurring at particular frequencies. Figure 4 illustrates the behaviour of the condition number in a number of other geometrical arrangements consisting of two sources, but with three, four and five microphones. Oscillations in the condition number still occur, although the peaks in condition number become less pronounced as the number of sensors is increased. Note however, that a large peak always occurs in the low frequency limit. It is interesting to observe that in the particular case of two sources and two sensors arranged symmetrically,

such that $r_{11} = r_{22} = r_{ms}$ and $r_{12} = r_{21} = r_c$, then in the low frequency limit (when $kS \rightarrow 0$ in equation (50)) the condition number becomes

$$\kappa(\mathbf{H}) = \frac{r_c + r_{ms}}{r_c - r_{ms}} \quad . \tag{51}$$

This also suggests that as the sensors are moved further from the sources, such that $r_c - r_{ms}$ becomes much smaller than $r_c + r_{ms}$, then the low frequency limiting value of $\kappa(\mathbf{H})$ increases. Similarly, decreasing the spacing between sources and spacing between sensors will have a detrimental effect on the condition number.

The effect of geometry on the condition number of a more practical number of sources and sensors is illustrated in Figure 5. This shows the variation of condition number with non-dimensional frequency kr_{ss}, where r_{ss} is the distance between sources, and r_{ms}/r_{ss}, where r_{ms} is the distance between two linear arrays of equally spaced sources and sensors. The distance between sensors is assumed to be also equal to r_{ss}. The curves in Figure 5 illustrate the frequency dependence of the condition number for the values of r_{ms}/r_{ss} given by 0.5, 2, 3, 10 and 30. Clearly the matrix $\mathbf{H}$ becomes very poorly conditioned for values of r_{ms}/r_{ss} greater than 10. It is also obvious from these results that the conditioning of the problem is greatly improved if the measurement array is deployed close to the source distribution. In particular, the inevitable increase in condition number at low frequencies is far less for a measurement array close to the source array.

3.3 THE EFFECT OF SOURCE/SENSOR GEOMETRY ON CONDITION NUMBER

A comprehensive study of the influence of the geometric parameters on the condition number is presented in reference [26]. Here we will summarise the main findings of this work. Figures 6, 7 and 8 show the variation of condition number with a range of parameters for source/sensor geometries consisting respectively of linear arrays of six

sources and sensors, rectangular arrays of thirty-five sources and sensors and square arrays of one hundred sources and sensors. The dependence is shown on the following parameters;

(1) Non-dimensional frequency kr_{ss}, where r_{ss} is the distance between sources.

(2) Ratio (r_{ms}/r_{ss}) of source plane/sensor plane distance to distance between sources.

(3) Ratio (r_{mm}/r_{ss}) of distance between sensors to distance between sources.

(4) The eccentricity (e) which defines the displacement of the sensor array from a symmetric position relative to the sources.

First note that parts (b) of each of Figures 6–8 demonstrate the important point that, at the particular value of $kr_{ss} \approx 0.55$, the smallest condition number is produced when $r_{mm} = r_{ss}$ and $e = 0$, i.e. the distance between sensors is made equal to the distance between sources. This is particularly so when r_{ms}/r_{ss} is small (i.e. the sensors are close to the sources). Parts (c) and (d) of the figures also demonstrate the effect of the eccentricity e and show that the minimum values of condition number at $r_{mm} = r_{ms}$ are only increased by the displacement of the sensors from the symmetric position. This increase in condition number due to eccentricity is particularly pronounced in the case of a large number of sources and sensors.

Parts (e) of the figures emphasise that $r_{mm}/r_{ss} = 1$ produces a minimum in the condition number for all values of kr_{ss} less than about 2, these plots being produced for specific values of $r_{ms}/r_{ss} = 1$. Finally, parts (f) of the figures again illustrate the dependence of condition number on kr_{ss}, but for a range of values of r_{ms}/r_{ss}, again illustrating the increase of ill-conditioning as r_{ms}/r_{ss} is increased when $e = 0$.

Figure 9 shows the variation of condition number with kr_{ss} for a range of models having increasing numbers of sources and sensors. In all cases $r_{mm}/r_{ss} = 1$ and $r_{ms}/r_{ss} = 1$ and $e = 0$. The plot clearly shows the steady increase of condition number with the increase in the number of sources and sensors used.

Finally, reference [26] describes a series of simulations which investigate the effect of using different sensor array geometries with a given source array geometry. Five different source arrays were chosen (two orthogonal line arrays, a cross array, an X array, and a square array) and in each case the condition number was evaluated for five different sensor arrays. The consistent finding of these studies was that the condition number was minimised when the geometry of the sensor array exactly matched the geometry of the source array. Two examples are shown in Figures 10 and 11. A remarkable reduction in condition number is afforded by matching the geometry of the sensor array to the geometry of the source array.

In summary, therefore, the acoustical inverse problem appears to be best conditioned when the number of sources and sensors is small, when the geometrical arrangement of sensors closely matches the assumed source array geometry, when the distance between sources is the same as the distance between sensors, when the sensor array is placed close to the source array and when the sensor array is positioned symmetrically with respect to the source array.

4. LIMITS TO RESOLUTION WITH THE IMPROVEMENT OF CONDITIONING

4.1 SIMULATIONS OF THE EFFECT OF SINGULAR VALUE DISCARDING AND TIKHONOV REGULARISATION ON SOURCE RESOLUTION

Following the establishment of general guidelines on the conditioning of the inverse problem, we will now demonstrate how effectively the use of singular value discarding can help retrieve useful solutions for the strength of acoustic sources, despite ill-conditioning of the matrix to be inverted. A series of simple simulations can be used to demonstrate the main features of the approach. The geometry dealt with is illustrated in Figure 5 and consists of linear arrays of nine sources and sensors. For the purpose of this exercise it is

assumed that the central source in the array has a unit strength, whilst all the other sources are assumed to have a strength of zero.

Figure 12 shows the singular values of the matrix **H** for the range of geometries considered. Figure 13 shows a series of graphs depicting the distribution of source strength deduced from the simulated measured pressure field when the matrix **H** is inverted using singular value discarding. In computing these results it was assumed that kr_{ss} = 0.366 (i.e. a frequency of 200 Hz when r_{ss} = 0.1 m). The effects of different levels of noise were simulated by adding random numbers to the "true" pressure field computed for the assumed source distribution. Figure 13 shows results for 10% and 20% random noise and for four positions of the measurement array relative to the source array ($r_{ms} = 0.5r_{ss}$, $2r_{ss}$, $3r_{ss}$, and 30 r_{ss}). The columns of graphs in Figure 13 correspond respectively to the cases when none, one, three and five of the smallest singular values of the matrix **H** are discarded before computing the solution for the source strength vector $\mathbf{q}_o$.

With reference to the uppermost row of graphs in Figure 13, where r_{ms} = 0.05 m (r_{ms} = 0.5 r_{ss}) and the problem is well conditioned (see Figure 12), it is clear that progressively discarding the singular values of **H** gives a progressively poorer spatial resolution of the source strength distribution. Note that very close to the true value of $\mathbf{q}_o$ is recovered, even in the presence of noise, when the problem is well conditioned and no singular values are discarded. However, as the sensor array is moved further from the source array and the conditioning worsens (Figure 12), discarding singular values improves the source strength estimate but at the expense of a decrease in spatial resolution. Thus, for example, in the case of $r_{ms} = 30r_{ss}$ (the fourth row of graphs in Figure 13(a)) it can be seen that when no singular values are discarded (the graph in the left-most column) the magnitude of the source strength estimate is seriously in error. This is also true of the graphs in the second and third columns, which correspond respectively to the cases where one and three singular values have been discarded. However, once five singular values have been discarded (in the case of the graph in the right-most column), at least the correct

order of magnitude of source strength is recovered, although the true source is very poorly resolved spatially. The results shown in Figure 13(b), which correspond to the case where 20% noise is added to the true values, show very similar trends to those of Figure 13(a) which correspond to the addition of 10% noise.

Figure 14 shows the result of Tikhonov regularisation of the solution, again for the addition of 10% and 20% noise. Very similar effects are observed to those associated with singular value discarding; the solution when appropriately regularised is capable of retrieving an estimate of the source strength magnitude which is at least of the correct order even if the source strength distribution is not well resolved spatially. It also becomes apparent that choosing too high a value of the regularisation parameter β results in even poorer resolution and poorer estimates of the source strength magnitude (see the results in the right-most column of Figure 14). We will return to the choice of an optimal value for β in a later report.

4.2 INTERPRETATION OF RESOLUTION LIMIT IN TERMS OF THE GENERALISED WAVENUMBER TRANSFORM

The results presented above can be understood by making reference to the interpretation given by previous workers [11, 12, 13, 14] to the SVD when used in connection with acoustic radiation problems. First recall that the relationship between the vector of radiated pressures $\mathbf{p}$ and the vector of acoustic source strengths $\mathbf{q}$ can be expressed in terms of the SVD of the transfer function matrix $\mathbf{H}$ such that

$$\mathbf{p} = \mathbf{U} \sum \mathbf{V}^H \mathbf{q} \ . \tag{52}$$

Now note that since the unitary matrix $\mathbf{U}$ has the property $\mathbf{U}^{-1} = \mathbf{U}^H$, then premultiplication of both sides of this equation by $\mathbf{U}^{-1}$ results in

$$\mathbf{U}^H \mathbf{p} = \Sigma \mathbf{V}^H \mathbf{q} \ . \tag{53}$$

We may now interpret $\mathbf{U}^H \mathbf{p} = \tilde{\mathbf{p}}$ as the vector of transformed complex pressures and $\mathbf{V}^H \mathbf{q} = \tilde{\mathbf{q}}$ as the vector of transformed complex source strengths which are related by

$$\tilde{\mathbf{p}} = \Sigma \tilde{\mathbf{q}} \ . \tag{54}$$

That is to say, since Σ is a diagonal matrix of real singular values, each element of the vector of transformed pressures is simply related to the corresponding element of the vector of transformed source strengths, the singular values determining the extent to which a given transformed source strength results in the corresponding transformed radiated pressure. As pointed out previously by Veronesi and Maynard [11], Borgiotti [12] and Photiadis [13], the transform operation $\tilde{\mathbf{q}} = \mathbf{V}^H \mathbf{q}$ is somewhat analogous to a Fourier wavenumber transform (of, for example, the surface velocity distribution in a planar radiation problem) whilst the operation $\tilde{\mathbf{p}} = \mathbf{U}^H \mathbf{p}$ is a similar transform of the pressure field (analogous to the Fourier wavenumber transform of radiated pressure in the planar radiation problem). The analogy between this transformation process and that used in planar NAH cannot, however, be pushed too far. The essence of planar NAH is the clear relationship between a given spatial Fourier component of the surface velocity distribution and the corresponding spatial Fourier component in the radiated field pressure; such components either propagate or decay exponentially with distance from the source. In the more general transformation process associated with the SVD it should be noted that the transformation process itself varies with "distance from the source"; the elements of the matrices $\mathbf{U}$ and $\mathbf{V}$ are determined entirely by source/sensor geometry and the transformed pressures and source strengths are related by a single real number (the singular value) which again specifically depends upon geometry.

This transformation process can perhaps be better understood by observing the elements of the matrices U and V for the nine source/nine sensor model investigated above. Figure 15 shows the elements of the matrices $\mathbf{U}^H$ and $\mathbf{V}^H$ for the particular value $r_{ms} = 3$ m (i.e. $r_{ms}/r_{ss} = 30$) of distance of the sensor array from the source array and for the non-dimensional frequency $kr_{ss} = 0.183$. Note that the rows of $\mathbf{U}^H$ and $\mathbf{V}^H$ define the set of orthonormal basis functions which are at the heart of the transformation process. The spatial distribution of these functions is clear. Note that the rows have been plotted in order of descending singular value and that, at least in this case, the "low spatial frequencies" are associated with large singular values whilst the "high spatial frequencies" are associated with small singular values. A similar plot is shown in Figure 16, but in this case, the source/sensor distance has been reduced to $r_{ms} = 0.3$ m (i.e. $r_{ms}/r_{ss} = 3$) although $k\, r_{ss}$ remains the same as for the case illustrated in Figure 15. Again it is the low spatial frequencies that are associated with the large singular values, although it should be noted that the form of the orthogonal basis functions differs from those illustrated in Figure 15, emphasising the geometry specific nature of the transformation process.

It is therefore evident that in the case studied above, the small singular values are associated with high spatial frequencies. Thus, for example, discarding these small singular values in the process of generating an acceptable solution to the inverse problem, inevitably leads to a deterioration in the spatial resolution of the inversion technique; the reconstructed results following the process of singular value discarding are inevitably a "spatially low pass filtered" version of the true source distribution. Whilst it is difficult to be general and each source/sensor geometry must be considered on its own merits, these observations are entirely consistent with the known behaviour of, for example, planar NAH, which requires close deployment of the measurement array in order to capture the evanescent field associated with high spatial frequencies in the source distribution. Measurement arrays deployed far from the source have an intrinsically limited spatial resolution.

5. CONCLUSIONS

The conditioning of the discrete inverse problem in acoustics is shown to be highly dependent on the geometry of sources and measurement positions and the frequency of the radiated sound. In particular, the problem generally becomes badly conditioned in the low frequency limit when the wavelength of the radiated sound becomes large compared to the distance between the sources. However, the conditioning of the problem generally becomes improved when the measurements are made at positions close to the acoustic sources and when the geometry of the measurement positions is chosen to "match" the geometry of the source array. Techniques such as Tikhonov regularisation and singular value discarding are shown to be useful methods for improving the accuracy of source strength reconstruction when the problem is poorly conditioned. Methods for choosing the regularisation parameter or the singular values to be discarded will be described in a later report. A further report will describe techniques for efficiently dealing with acoustic sources whose strengths are a time stationary random processes when measurement of the matrix of cross spectra of radiated acoustic pressures are required. A report describing the experimental application of these techniques will also be presented.

REFERENCES

1. B.D. VAN VEEN and K.M. BUCKLEY 1998 *IEEE ASSP Magazine*, 4-24. Beamforming: A versatile approach to spatial filtering.
2. J. BILLINGSLEY and R. KINNS 1976 *Journal of Sound and Vibration* **48**, 485-510. The acoustic telescope.
3. M.J. FISHER, M. HARPER-BOURNE, S.A.L. GLEGG 1977 *Journal of Sound and Vibration* **51**, 23-54. Jet engine noise source location: the polar correlation technique.

4. J.D. MAYNARD, E.G. WILLIAMS and Y. LEE 1985 *Journal of the Acoustical Society of America* **78**, 1395-1413. Nearfield acoustic holography: I. Theory of generalised holography and the development of NAH.

5. W.A. VERONESI and J.D. MAYNARD 1989 *Journal of the Acoustical Society of America* **85**, 588-598. Digital holographic reconstruction of sources with arbitrarily shaped surfaces.

6. J. HALD 1989 *Brüel and Kjær Technical Review No 1.* STSF-a unique technique for scan-based Near-field Acoustic Holography without restrictions on coherence.

7. J. HALD 1995 *Brüel and Kjær Technical Review No 1.* Spatial transformation of sound fields (STSF) techniques in the automotive industry.

8. K.B. GINN and J. HALD 1989 *Brüel and Kjær Technical Review No 2.* STSF-practical instrumentation and application.

9. B.J. TESTER and M.J. FISHER 1991 *AIAA 7th Aeroacoustics Conference, Palo Atto, California, USA, AIAA-81-2040.* Engine noise source breakdown: Theory, simulation and results.

10. P.J.T. FILLIPI, D. HABAULT and J. PIRAUX 1988 *Journal of Sound and Vibration* **124**, 285-296. Noise source modelling and identification procedure.

11. W.A. VERONESI and J.D. MAYNARD 1989 *Journal of the Acoustical Society of America* **85**, 588-598. Digital holographic reconstruction of sources with arbitrarily shaped surfaces.

12. G.V. BORGIOTTI 1990 *Journal of the Acoustical Society of America* **88**, 1884-1893. The power radiated by a vibrating body in an acoustic fluid and its determination from boundary measurements.

13. D.M. PHOTIADIS 1990 *Journal of the Acoustical Society of America* **88**, 1152-1159. The relationship of singular value decomposition to wave-vector filtering in sound radiation problems.

14. S.J. ELLIOTT and M.E. JOHNSON 1993 *Journal of the Acoustical Society of America* **94**, 2194-2204. Radiation modes and the active control of sound power.

15. G.T. KIM and B.H. LEE 1990 *Journal of Sound and Vibration* **136**, 245-26. 3-D sound reconstruction and field projection using the Helmholtz integral equation.

16. R. STOUGHTON and S. STRAIT 1993 *Journal of the Acoustical Society of America* **94**, 827-834. Source imaging with minimum mean-squared error.

17. S.P. GRACE, H.M. ATASSI and W.K. BLAKE 1996 *AIAA Journal* **34**, 2233-2240. Inverse aeroacoustic problem for a streamlined body, Part 1: Basic formulation.

18. S.P. GRACE, H.M. ATASSI and W.K. BLAKE 1996 *AIAA Journal* **34**, 2241-2246. Inverse aeroacoustic problem for a streamlined body, Part 2: Accuracy of solutions.

19. M.J. FISHER and K.R. HOLLAND *Journal of Sound and Vibration* **201**, 103-125. Measuring the relative strengths of a set of partially coherent acoustic sources.

20. G.H. GOLUB, M. HEATH and G. WAHBA 1979 *Technometrics* **21**, 215-223. Generalized cross-validation as a method for choosing a good ridge parameter.

21. P.A. NELSON and S.J. ELLIOTT 1992 *Active Control of Sound*, Academic Press, London, 416-420.

22. G.H. GOLUB and C.F. VAN LOAN *Matrix computations*, Second Edition, The John Hopkins University Press, Bathmore.

23. S.J. ELLIOTT, C.C. BOUCHER and P.A. NELSON 1992 *IEEE Transactions on Signal Processing* **40**, 1041-1052. The behaviour of a multiple channel active control-system.

24. F. DEPRETTERE 1988 *SVD and Signal Processing*, North Holland, Amsterdam.

25. S.H. YOON and P.A. NELSON 1995 *ISVR Technical Memorandum 779, University of Southampton.* Some techniques to improve stability in identifying acoustic source strength spectra.

26. S.H. YOON and P.A. NELSON 1997 *ISVR Technical Memorandum 817, University of Southampton.* On the condition number of the matrix to be inverted in an acoustic inverse problem.

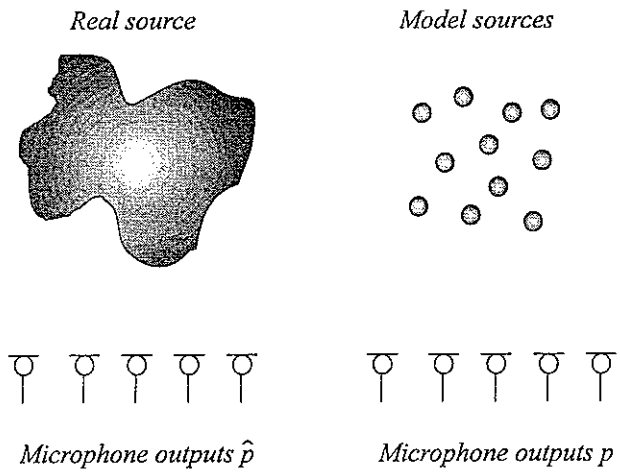

Figure 1. Schematic of the model based approach to source strength estimation.

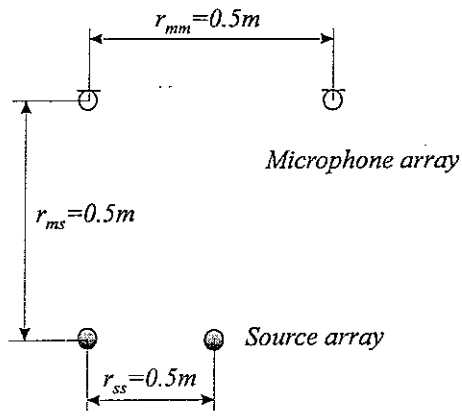

Figure 2. A geometrical arrangement of 2 sources and 2 microphones.

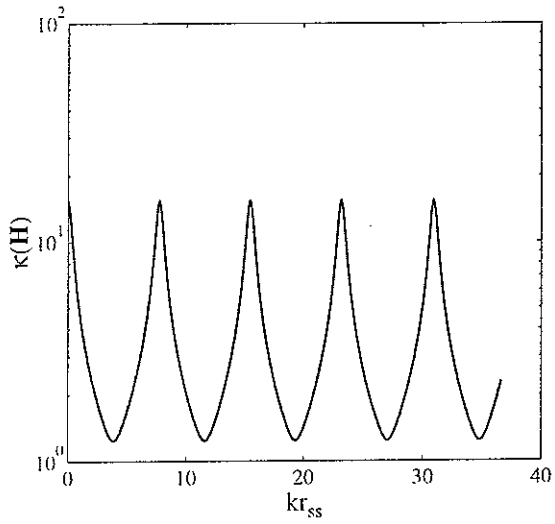

Figure 3. Condition number of the matrix **H** of the model consisting of 2 sources and 2 microphones as shown in Figure 2.

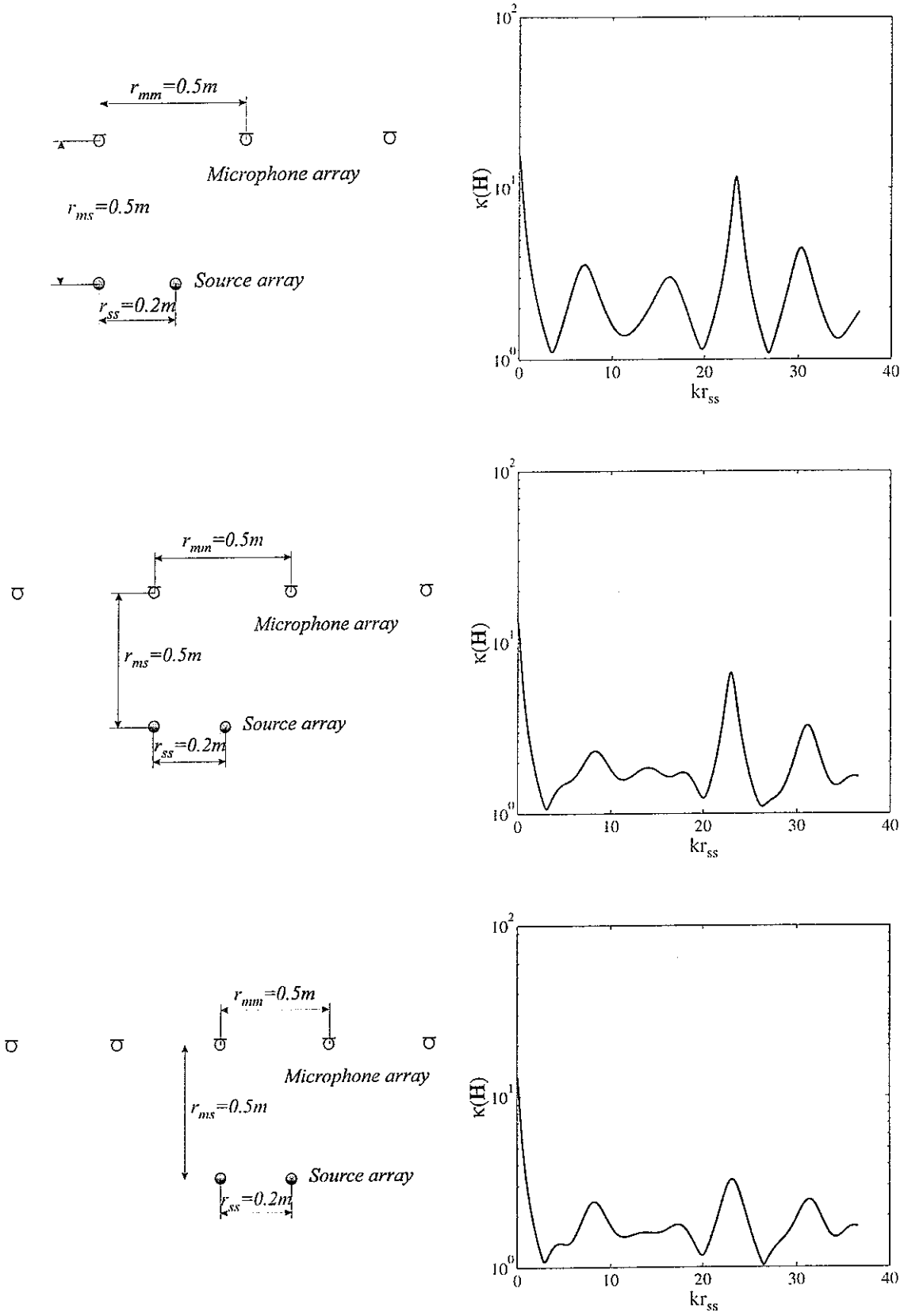

Figure 4. The condition number of the matrix **H** for some geometrical arrangements of sources and microphones.

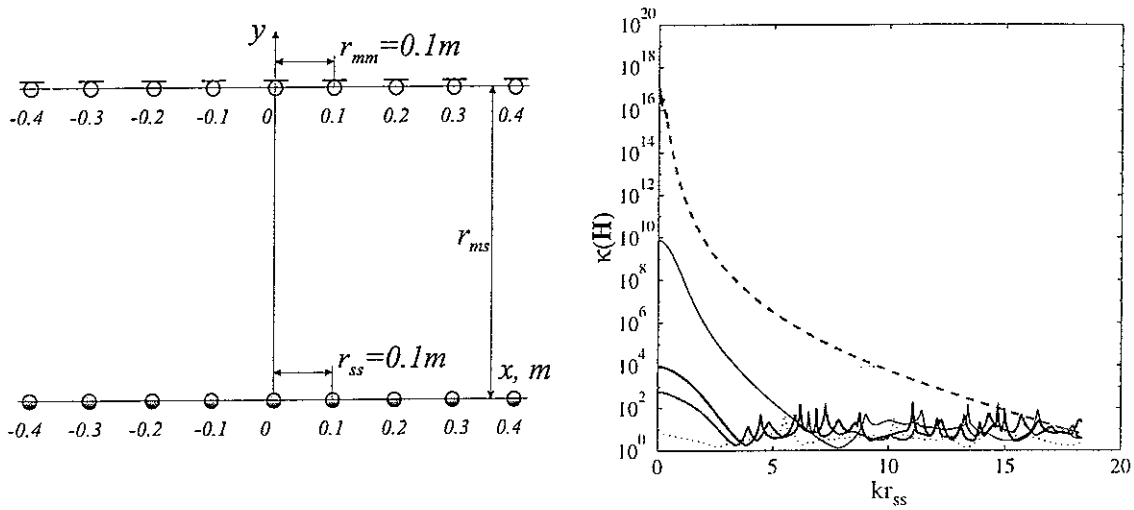

Figure 5. Variation of the condition number of the matrix **H** with the ratio r_{ms}/r_{ss}: dotted: r_{ms}/r_{ss} =0.5, gray solid: r_{ms}/r_{ss} =2, black solid: r_{ms}/r_{ss} =3, thin solid: r_{ms}/r_{ss} =10, gray dashed: r_{ms}/r_{ss} =30.

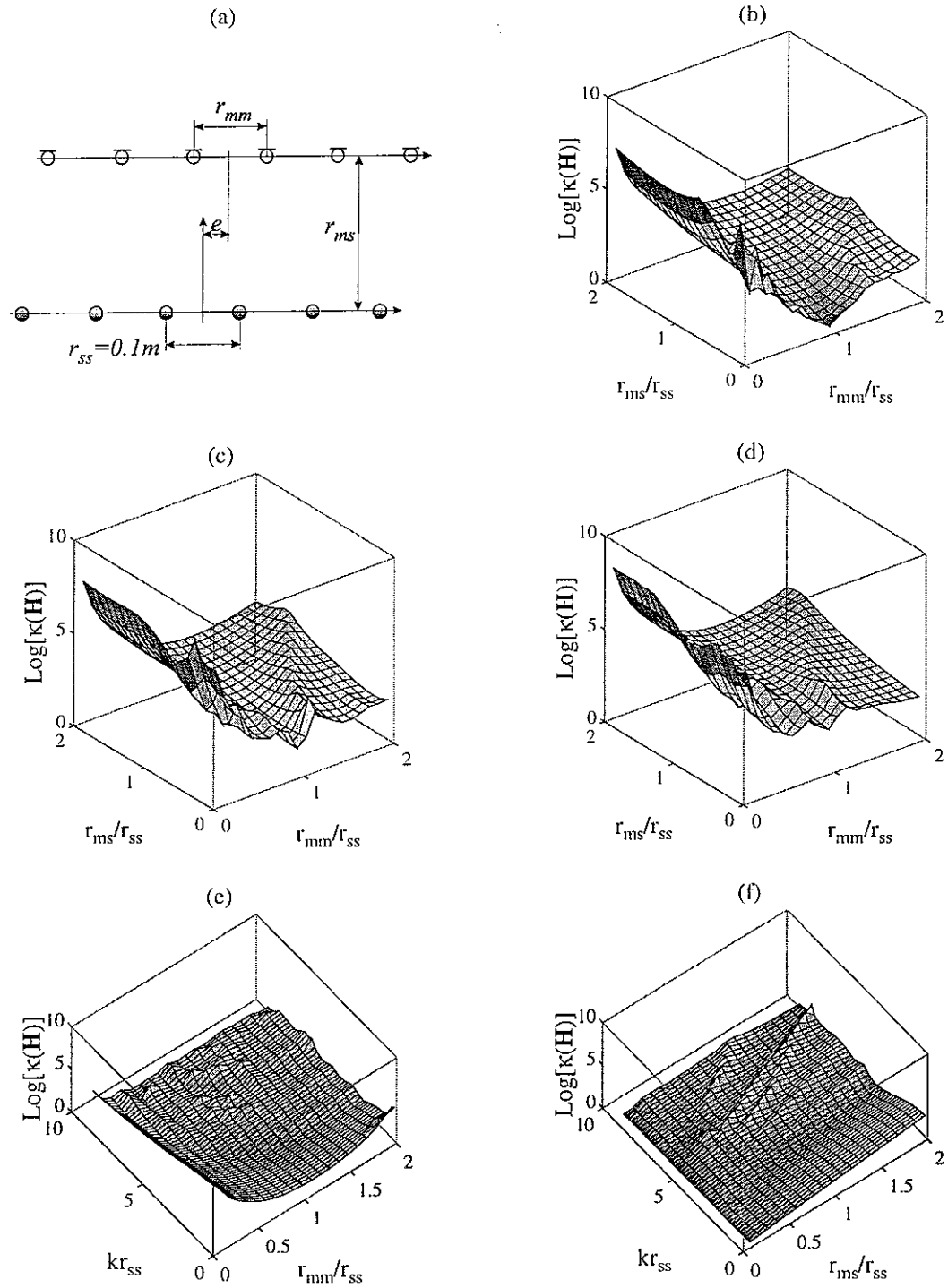

Figure 6. (a) A geometrical arrangement of 6 sources and 6 microphones. Variation of the condition number $\kappa(\mathbf{H})$: (b) $kr_{ss}\approx 0.55$ (=300Hz), e=0, (c) $kr_{ss}\approx 0.55$ (=300Hz), e=-0.5r_{ss}, (d) $kr_{ss}\approx 0.55$ (=300Hz), e=0.8r_{ss}, (e) r_{ms}/r_{ss}=1, e=0, (f) r_{mm}/r_{ss}=1, e=0.

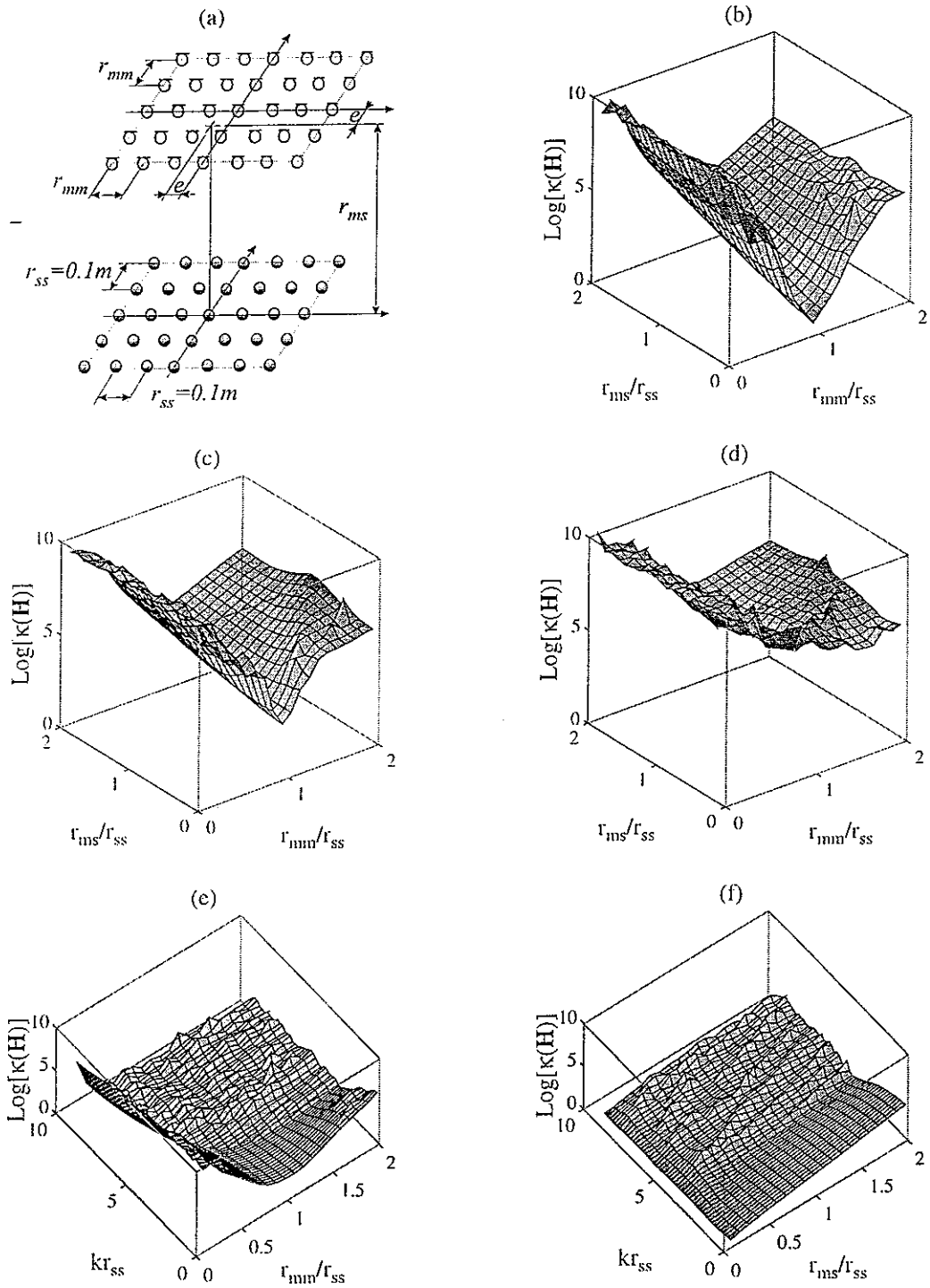
(a)
r_{mm}
r_{mm}
e
e
r_{ms}
r_{ss}=0.1m
r_{ss}=0.1m
(b)
Log[κ(H)]
10
5
0
2
1
0 0
1
2
r_{ms}/r_{ss}
r_{mm}/r_{ss}
(c)
Log[κ(H)]
10
5
0
2
1
0 0
1
2
r_{ms}/r_{ss}
r_{mm}/r_{ss}
(d)
Log[κ(H)]
10
5
0
2
1
0 0
1
2
r_{ms}/r_{ss}
r_{mm}/r_{ss}
(e)
Log[κ(H)]
10
5
0
10
5
0 0
0.5
1
1.5
2
kr_{ss}
r_{mm}/r_{ss}
(f)
Log[κ(H)]
10
5
0
10
5
0 0
0.5
1
1.5
2
kr_{ss}
r_{ms}/r_{ss}

Figure 7

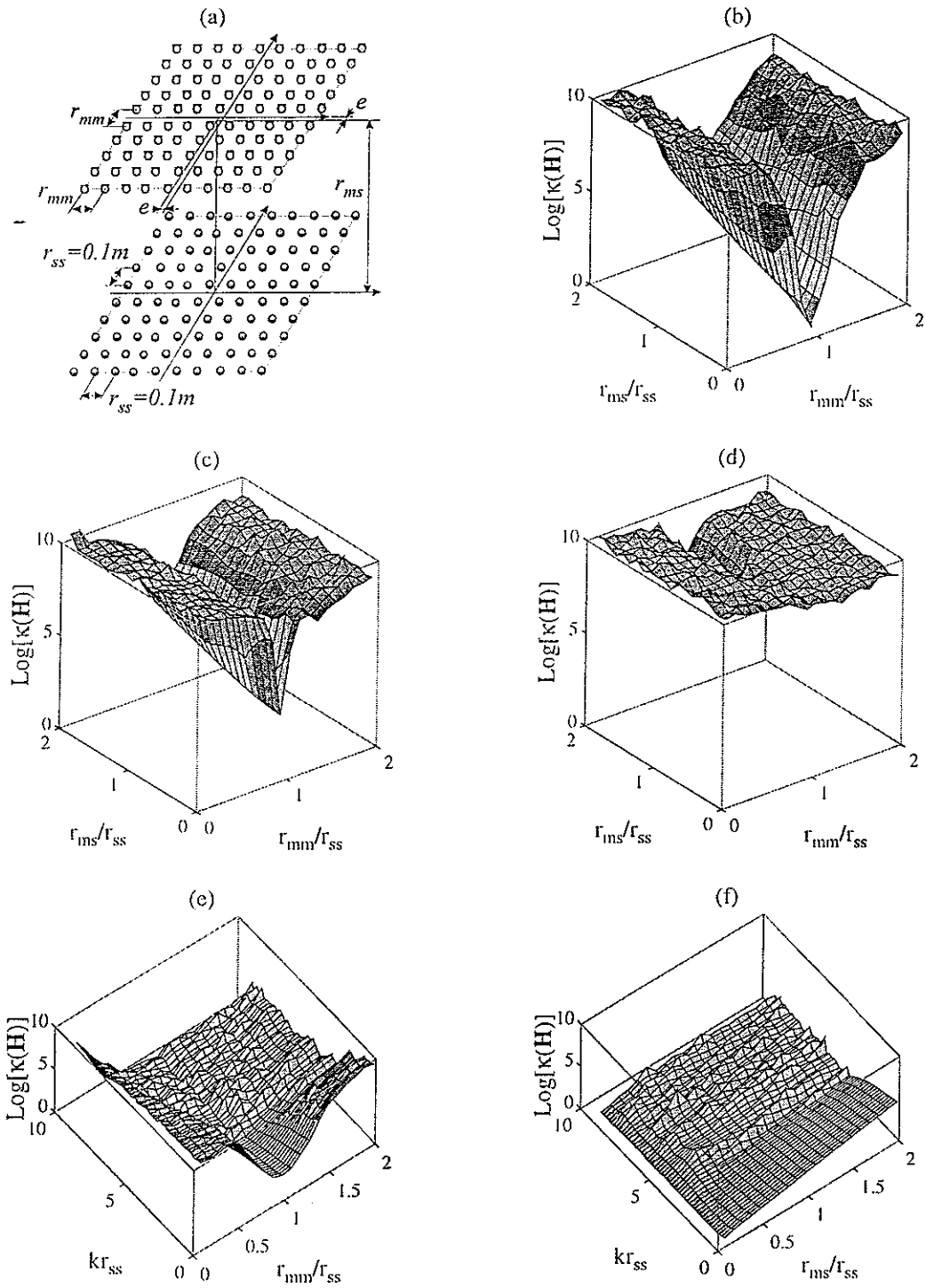
(a)
r_{mm}
e
r_{ms}
r_{mm}
e
r_{ss}=0.1m
r_{ss}=0.1m
(b)
Log[κ(H)]
10
5
0
2
1
0 0
1
2
r_{ms}/r_{ss}
r_{mm}/r_{ss}
(c)
Log[κ(H)]
10
5
0
2
1
0 0
1
2
r_{ms}/r_{ss}
r_{mm}/r_{ss}
(d)
Log[κ(H)]
10
5
0
2
1
0 0
1
2
r_{ms}/r_{ss}
r_{mm}/r_{ss}
(e)
Log[κ(H)]
10
5
0
10
5
0 0
0.5
1
1.5
2
kr_{ss}
r_{mm}/r_{ss}
(f)
Log[κ(H)]
10
5
0
10
5
0 0
0.5
1
1.5
2
kr_{ss}
r_{ms}/r_{ss}

Figure 8

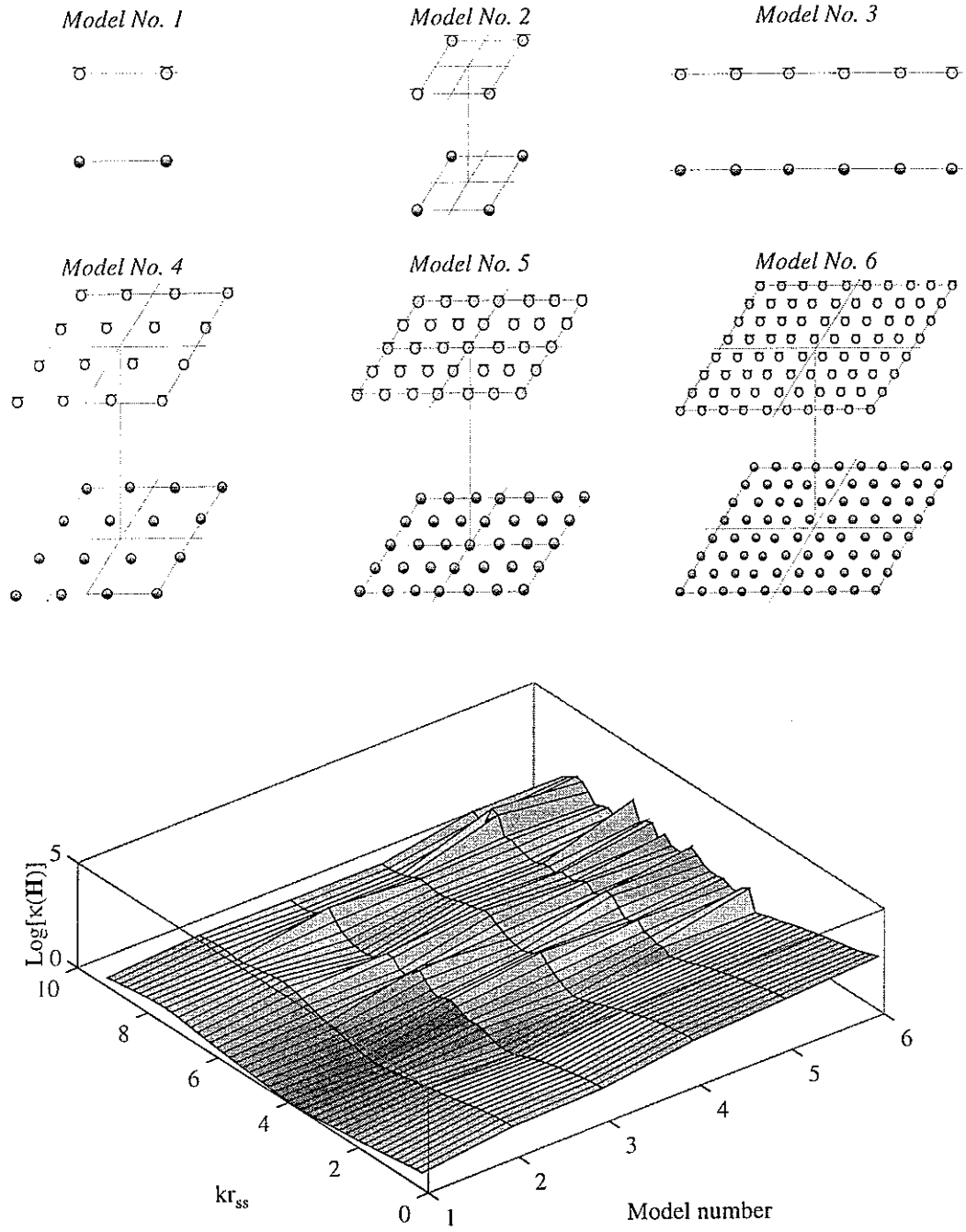

Figure 9. A comparison of condition numbers $\kappa(\mathbf{H})$ of 6 models: $r_{ss}=r_{mm}=r_{ms}=0.1$m, and the microphone array is placed symmetrically with respect to the source array (i.e., $e=0$).

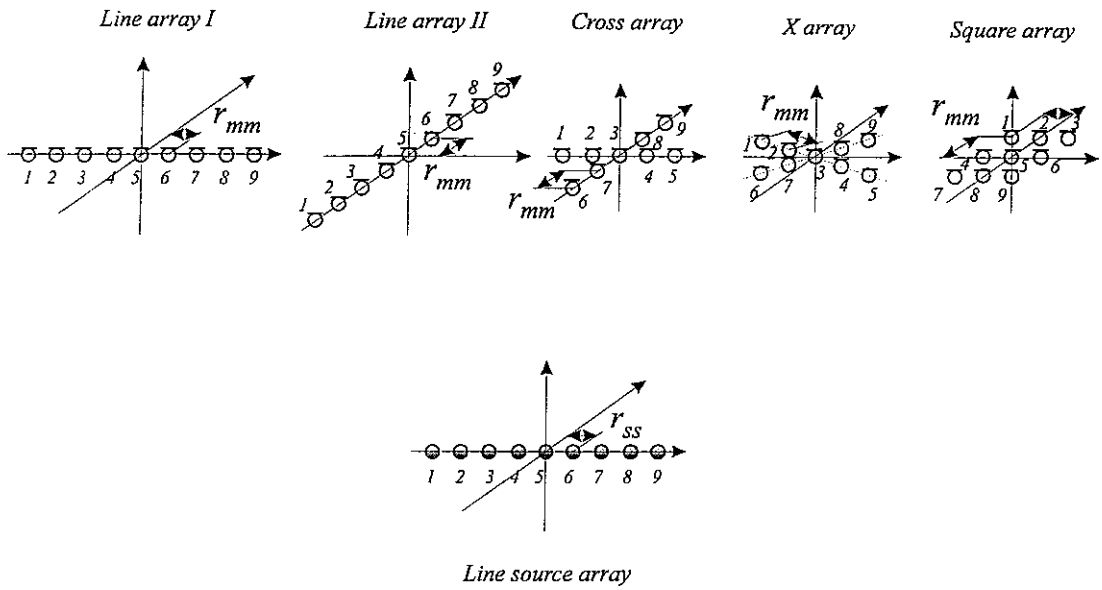

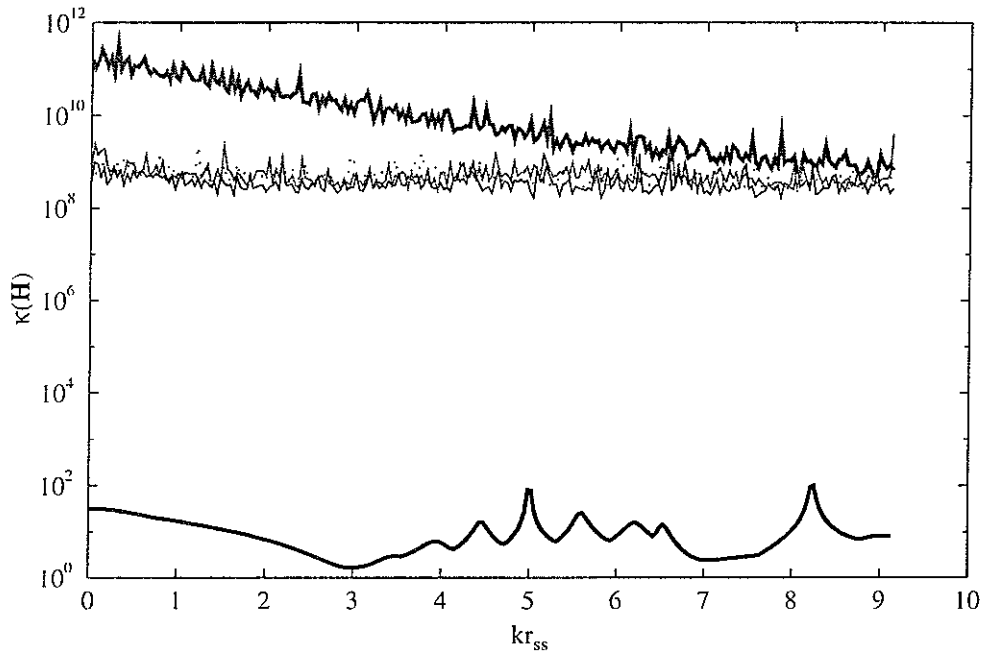

Figure 10. Condition numbers for the five different types of microphone array when used with the line source array. Black thick solid: line microphone array I, gray thick solid: line microphone array II, black thin: cross mocrophone array, gray thin: x microphone array, dotted: square microphone array.

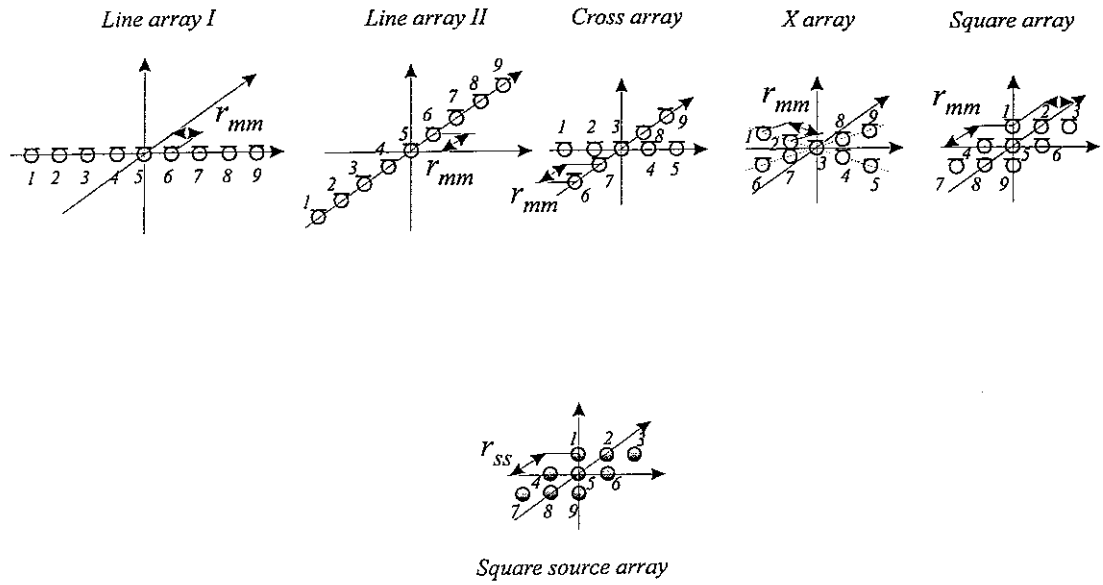

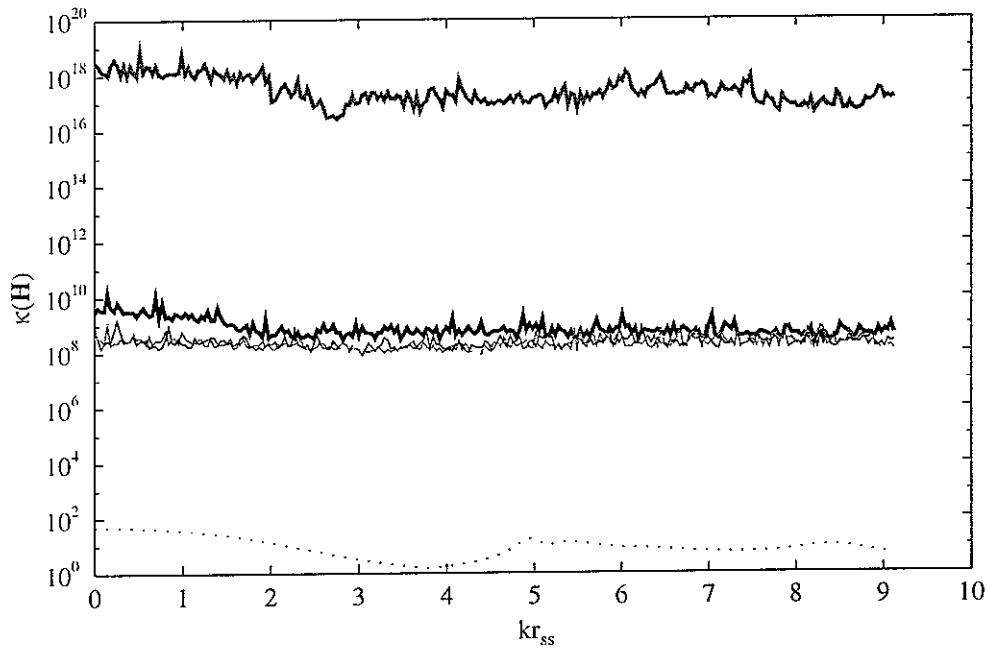

Figure 11. Condition numbers for the five different types of microphone array when used with the square source array. Black thick solid: line microphone array I, gray thick solid: line microphone array II, black thin: cross microphone array, gray thin: x microphone array, dotted: square microphone array.

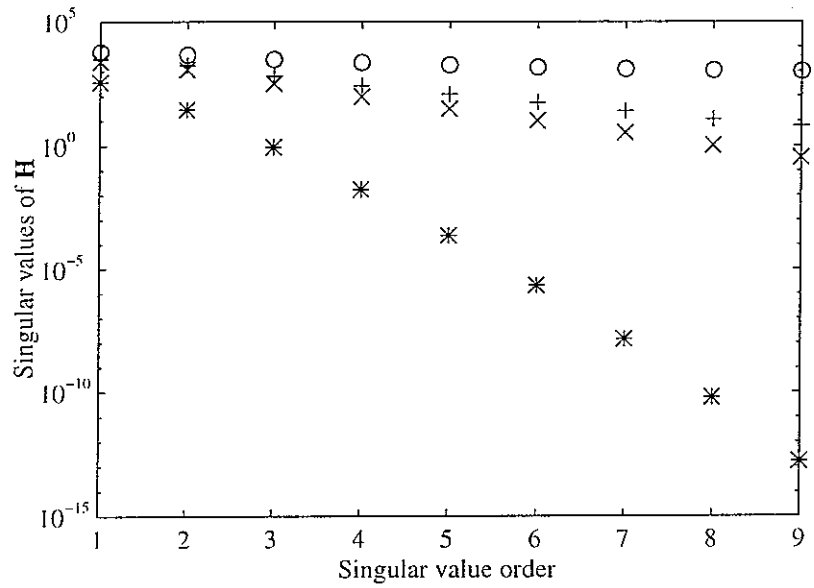

Figure 12. Singular values of the matrix **H** for the model of Figure 5: circle: $r_{ms}=0.5r_{ss}$ ($\kappa(\mathbf{H})=5.90$), plus: $r_{ms}=2r_{ss}$ ($\kappa(\mathbf{H})=5.06\text{x}10^{2}$), x-mark: $r_{ms}=3r_{ss}$ ($\kappa(\mathbf{H})=7.50\text{x}10^{3}$), star: $r_{ms}=30r_{ss}$ ($\kappa(\mathbf{H})=2.16\text{x}10^{15}$).

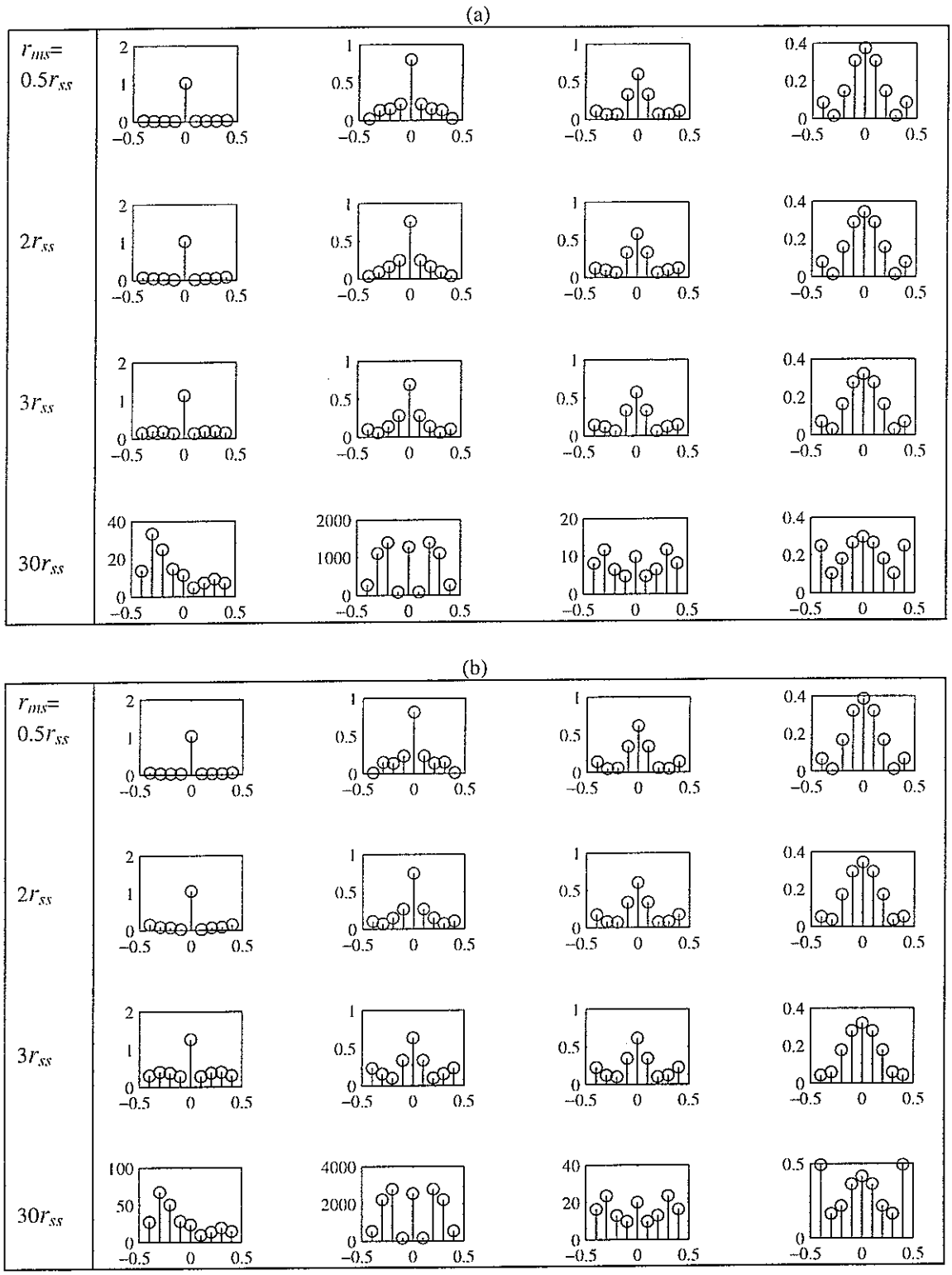

Figure 13. Resolution capability of the singular value discarding technique for the 9 monopole source and 9 microphone model (Figure 5) with the change of the distance r_{ms} and the singular values discarded. Graphs show the magnitude of $\mathbf{q}_o$ (m^3/s^{-1}) as a function of position x (m) (1st column: discarding no singular value, 2nd column: discarding the last singular value, 3rd column: discarding the last 3 singular values, 4th column: discarding the last 5 singular values): kr_{ss}=0.366 (=200Hz): (a) 10% noise, (b) 20% noise.

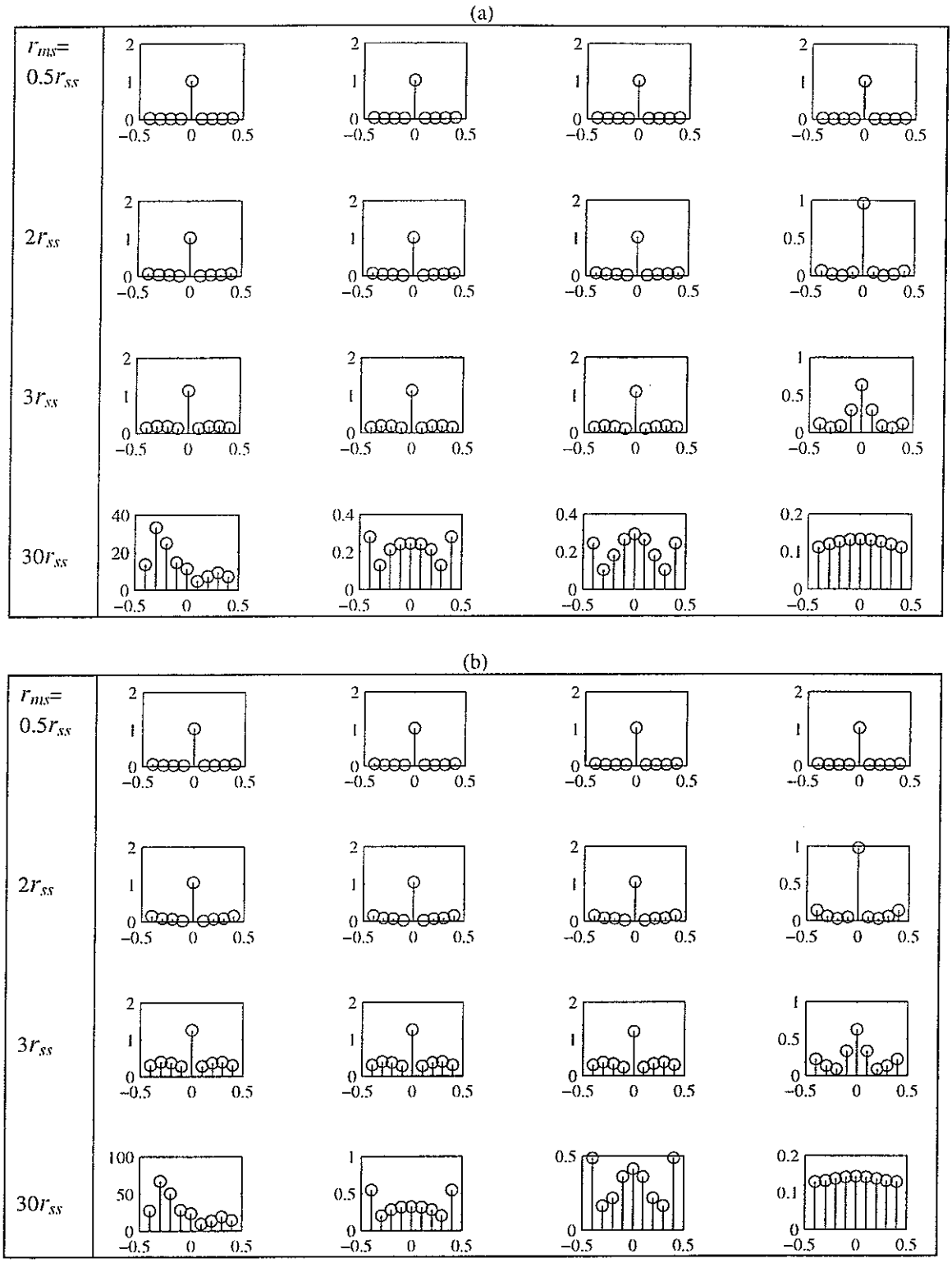

Figure 14. Resolution capability of the Tikhonov regularisation technique for the 9 monopole source and 9 microphone model (Figure 5) with the change of the distance r_{ms} and the regularisation parameter. Graphs show the magnitude of $\mathbf{q}_o$ (m^3/s^{-1}) as a function of position x (m). (1st column: β=0, 2nd column: β=1x10^{-5}, 3rd column: β=1x10^{-2}, 4th column: β=10): kr_{ss}=0.366 (=200Hz): (a) 10% noise, (b) 20% noise.

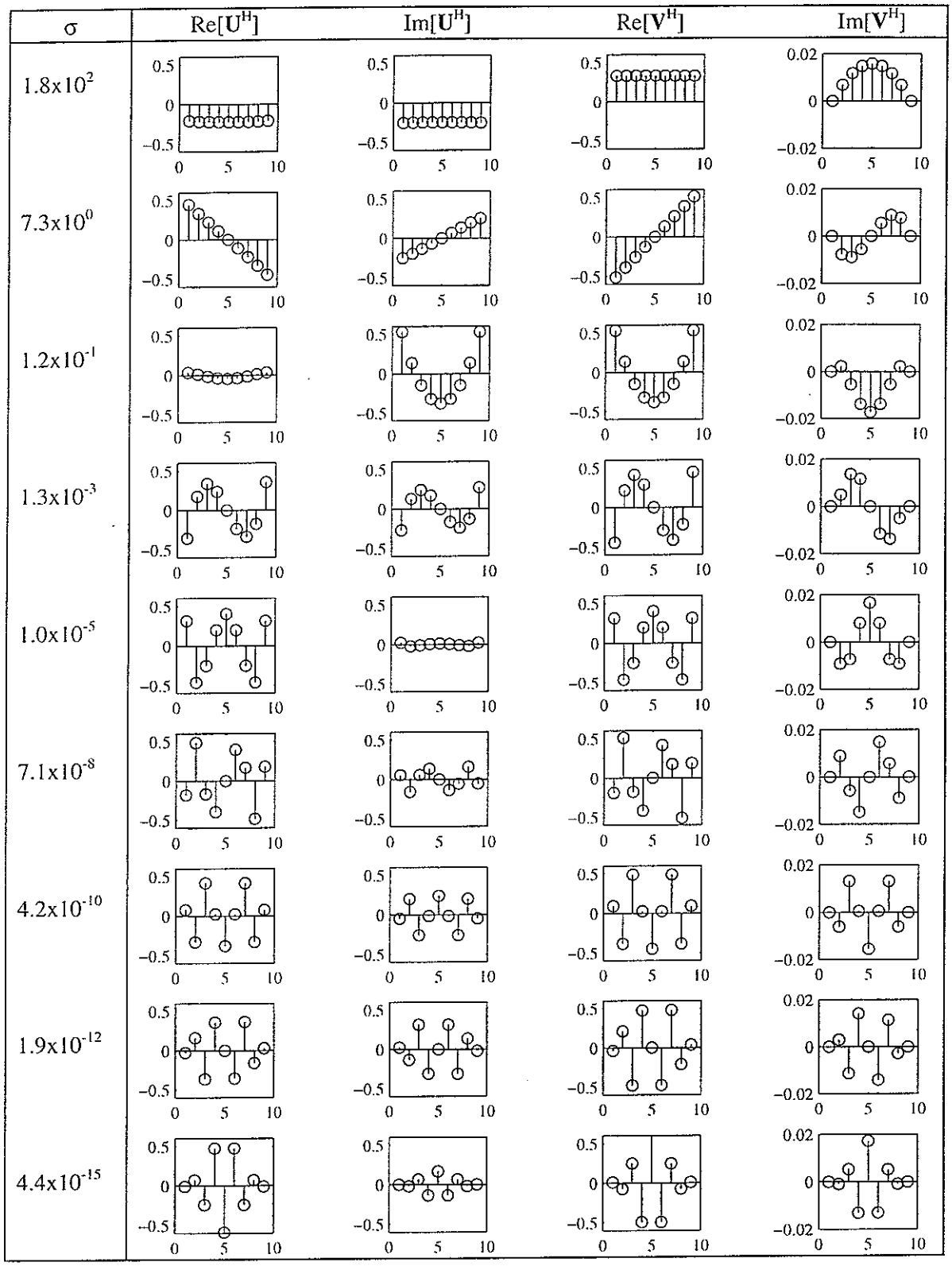

Figure 15. Row elements of the matrices $\mathbf{U}^H$ and $\mathbf{V}^H$ for the source/sensor geometry illustrated in Figure 5 with r_{ms}=3m (r_{ms}/r_{ss}=30) and kr_{ss}=0.183 (100Hz). The left hand column shows the singular values of $\mathbf{H}$ corresponding to the rows of $\mathbf{U}^H$ and $\mathbf{V}^H$.

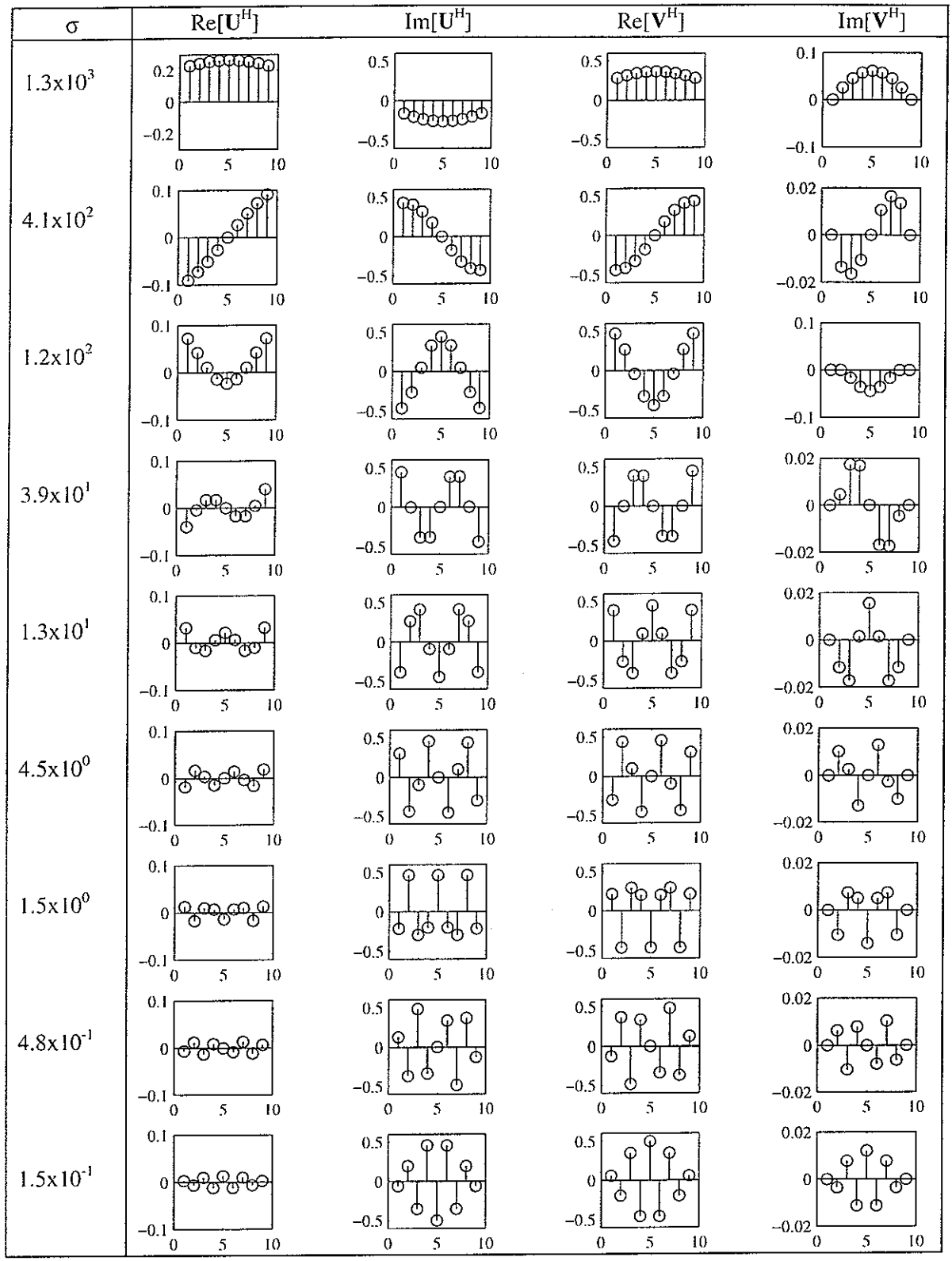

Figure 16. Row elements of the matrices $\mathbf{U}^H$ and $\mathbf{V}^H$ for the source/sensor geometry illustrated in Figure 5 with r_{ms}=0.3m (r_{ms}/r_{ss}=3) and kr_{ss}=0.183 (100Hz). The left hand column shows the singular values of $\mathbf{H}$ corresponding to the rows of $\mathbf{U}^H$ and $\mathbf{V}^H$.